GENERAL INTRODUCTION

Marine algae have been used in many coastal regions, such as Japan, Korea and China, as foodstuffs, industrial products, and fertilizer. In recent years, there is an increasing concern about the utilization of algae based on their valuable chemical constituents, such as protein, dietary fiber, lipids and minerals, many of which exhibit multiple bioactivities with applications in the food and cosmetic (1-4). Carotenoids are natural compounds of particular interest in algae, and have recently received much consideration due to the many proposed health benefits such as antioxidant, anticancer, anti-inflammatory and anti-obesity activities (5). Algae generally contain many kinds of carotenoids, and some carotenoids are specific for algal divisions or classes (6) (**Fig. 1**). As antenna pigments of light harvesting processes, these specific carotenoids in particular algal groups have similar biological and ecological functions to terrestrial carotenoids. However, the specific carotenoids from algae have different biological merits in human health due to their specific structure, such as allenic bond, keto and epoxide groups (6). Therefore, current research aims to explore their biological benefits in human health and elucidate their functional mechanisms. Some studies provide valuable evidences that several marine carotenoids have beneficial effects on the obesity and obesity-associated metabolic syndrome. For instance, astaxanthin has been demonstrated to prevent high fat diet-induced obesity and hepatic steatosis in animal models (7, 8). Fucoxanthin, a major keto-carotenoid in brown algae, has been reported to possess anti-obesity properties in mice model and human subjects (9-12).

Siphonaxanthin with a keto group at C-8 and an additional hydroxyl group at C-19 was unique carotenoid found in green algae, such as *Caulerpa lentillifera*, *Codium fragile* and *Umbraulva japonica*, and euglenophyta. In the previous studies, potent anti-angiogenic effect of siphonaxanthin via down-regulation of FGF-2 signaling has been found by using

endothelial cell line and *ex vivo* angiogenesis model (13, 14). Siphonaxanthin has also been shown to possess more potent apoptosis-inducing effect in human leukemia cells compared with fucoxanthin (15). However, there has been no information about the effect of siphonaxanthin on obesity.

Obesity has reached pandemic proportions in recent years, which has resulted in increasing health care burden and decreasing life expectancy (16). Obesity, especially visceral obesity (**Fig. 2**), has been convincingly associated with insulin resistance, type 2 diabetes, hypertension and dyslipidemia, and leads to an increased risk of cardiovascular disease (17). Although several anti-obesity drugs have been reported to control obesity, most of those drugs have a significant concern about adverse effects (18). At present, a variety of natural compounds including some kinds of carotenoids, have gained attention due to their relative safety and accumulated evidences of their anti-obesity and anti-diabetic effects (19-21).

Furthermore, bioavailability and metabolism of the functional carotenoids *in vivo* concern exertion of their biological activates. It is reported that fucoxanthin could be metabolized to fucoxanthinol and amarouciaxanthin A in HepG2 cells and mice (22). And the metabolites of fucoxanthin have been suggested to be more effective in preventing obesity than fucoxanthin (23, 24). Regarding siphonaxanthin, however, no information is available about its bioavailability and biotransformation *in vivo*. Thus, it is necessary to assess bioavailability and metabolism of siphonaxanthin.

Considering the ever-increasing demand of nutraceuticals for prevention and improvement of obesity, in this study, for the first time, the anti-obesity effects of the green algal siphonaxanthin were evaluated, and the possible molecular mechanisms of siphonaxanthin were investigated. Furthermore, the metabolism and tissues distribution of dietary siphonaxanthin were also examined. In addition, the possible role of siphonaxanthin in the

anti-obesity effect of green algae was evaluated. This study would provide a possibility for new applications of green algal siphonaxanthin as functional food with anti-obesity property.

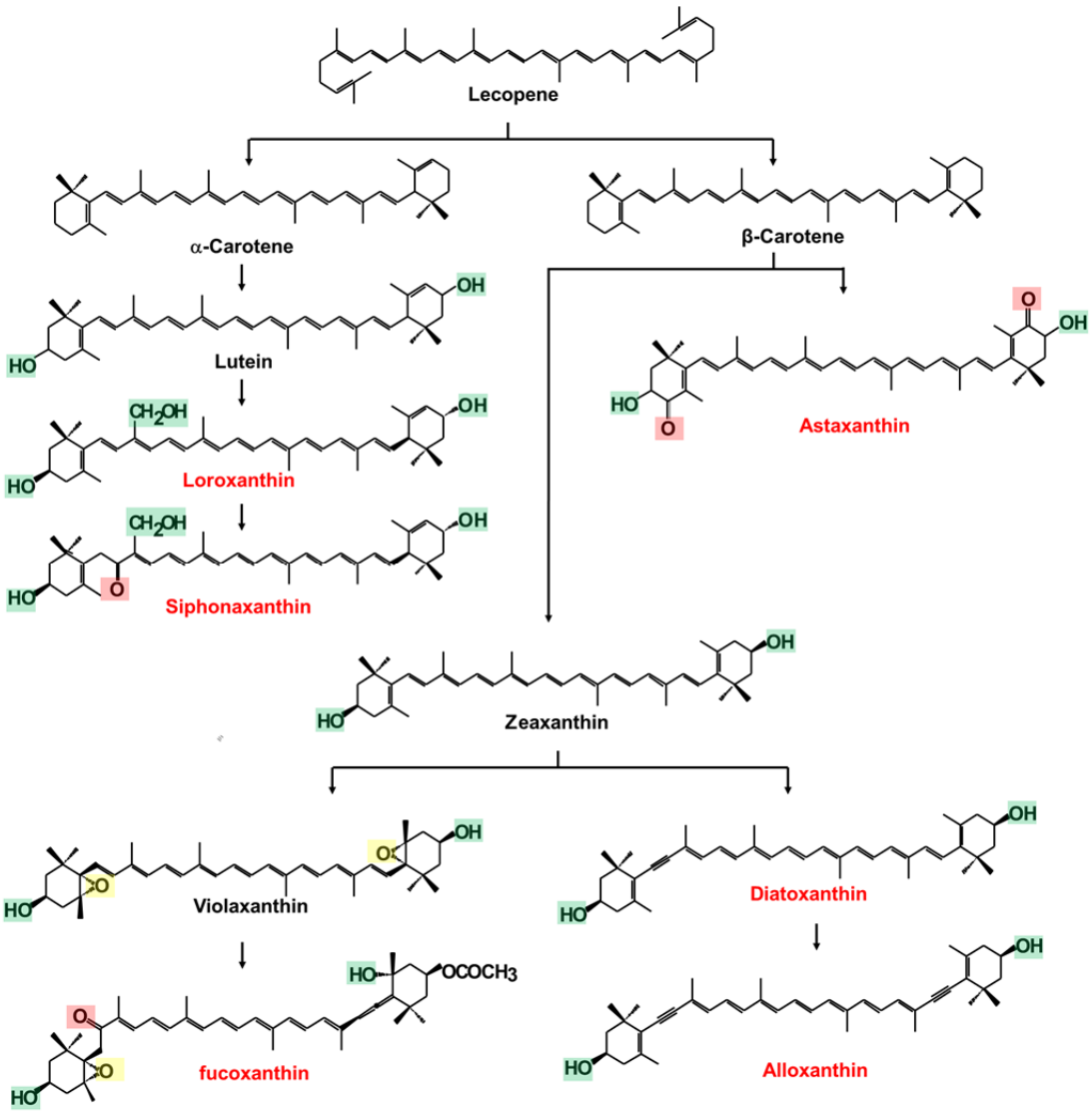

FIGURE 1 Carotenogenesis pathways in algae. Under a stressful environment, such as high light, UV irradiation and nutrition stress, several specific carotenoid, especially keto-carotenoids (fucoxanthin, astaxanthin, siphonaxanthin), are synthesized. Siphonaxanthin and loroxanthin could be considered to be derived from lutein, but the pathways and enzymes are still unknown.

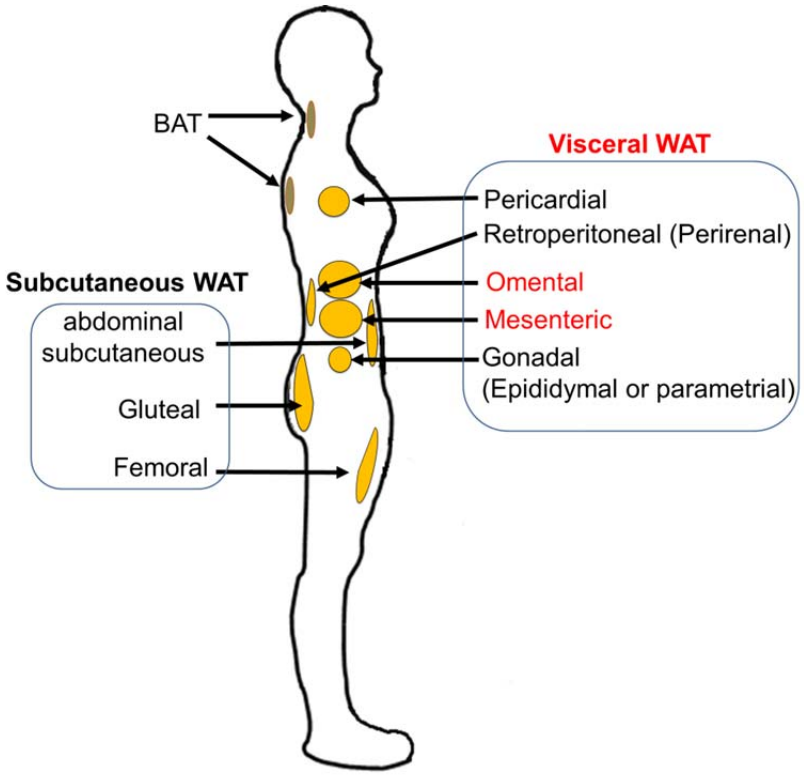

FIGURE 2 Distribution of adipose tissues in human body. The main white adipose tissues (WATs) **(25)** are abdominal subcutaneous adipose tissue, and visceral adipose tissue. Visceral adipose tissue surrounds the inner organs and can be divided in omental, mesenteric, retroperitoneal (surrounding the kidney), gonadal (attached to the uterus and ovaries in females and epididymis and testis in men), and pericardial. The omental depot distributes near the stomach and spleen, and can expand into the ventral abdomen, while the deeper mesenteric depot is attached in a web-form to the intestine. The gluteal and femoral adipose tissue is the subcutaneous WAT located to the lower-body parts and is measured by hip, thigh, and leg circumference. WAT can also be found intramuscularly. Brown adipose tissue (BAT) is found above the clavicle and in the subscapular region. Although the mentioned subcutaneous and visceral WAT are found in humans, perirenal and gonadal depots are mostly studied in rodents. The visceral WATs have been linked to risk of developing obesity-related diseases. The omental and mesenteric visceral WATs were found to be well-documented link to the risk.

INTRODUCTION

Worldwide, incidence of obesity has dramatically expanded over the last two decades due to the consumption of calorie-rich diet and the changes of lifestyle (26). The development of obesity involves extensive adipose tissue remodeling by hypertrophy and hyperplasia of adipocytes and angiogenesis (27). The dysregulations of adipocytes and adipose tissue function are associated with an increased risk of type 2 diabetes, cardiovascular diseases, hypertension, dyslipidemia, and some cancers (28). In adult humans, adipogenesis, the development of fat cells from preadipocytes, is responsible for adipocyte hyperplasia, and also contributes a compensatory replacement of adipocyte loss owing to an active adipocyte turnover in adipose tissue (29). Adipocytes reach maturity and become functional through adipogenesis, in which fibroblast-like preadipocytes differentiate into lipid-laden and insulin-responsive adipocytes (30, 31). This process occurs in several stages and requires an elaborate network of transcription factors, among which PPAR gamma (PPARG) and CCAAT/enhancer binding proteins (CEBPs) are considered the principal determinants of cell fate (32). In addition, numerous signaling pathways, including the insulin/IGF1 signaling pathway, are known to play vital roles in directing adipogenesis (33). The 3T3-L1 preadipocyte culture system, which recapitulates most of the critical aspects of fat cell formation *in vivo*, has been widely used as an *in vitro* model to study the molecular mechanisms regulating adipogenesis (34). Accordingly, the establishment of animal models is valuable to assess the efficacy of potential therapeutic agents in treatment of obesity. KK-Ay mice were established via transferring yellow obese gene (Ay) (35) into glucose-intolerant black KK mice. Under a regular chaw, the KK-Ay mice spontaneously become obese, hyperinsulinaemia and hyperglycemia (36). Therefore, the KK-Ay mouse has been considered as a useful animal model system to study pathogenesis, therapy, and prevention of obesity and diabetes (37).

In recent years, marine algae have served as a valuable source for functional compounds with potentially beneficial health effects. Among these compounds from marine algae, natural carotenoids have attracted a great deal of attention because of their diverse and beneficial bioactivities, such as antioxidant, anticancer, anti-inflammatory, and anti-obesity activities (5). Fucoxanthin, an extensively studied carotenoid from marine brown algae, has been reported to have remarkable anti-obesity properties, including decreased body weight gain and improved lipid metabolism in both obese mice (38, 39) and high-fat-diet induced obese mice (40, 41).

Siphonaxanthin is a xanthophyll present in green algae that can survive in the deep water，such as *Codium fragile*, *Codium cylindricum*, and *Umbraulva japonica* (6). It is previously found that siphonaxanthin possesses anti-angiogenic and apoptosis-inducing activities (13, 15), and that this beneficial effect may result from its inhibitory effects on various kinases, including protein kinase B (Akt) and extracellular signal-regulated kinase (ERK) (14). Siphonaxanthin is one of the oxidative metabolites of lutein, and its structure contains a conjugated system of eight C=C double bonds and one keto group located at C-8, similar to fucoxanthin (42). In addition to these structural groups, siphonaxanthin has an extra hydroxyl group at C-19 that might contribute it to be more beneficial than other carotenoids (15, 43). However, the potential role of siphonaxanthin in adipogenesis and its underlying mechanisms have not been studied.

In this chapter, the effect of siphonaxanthin on adipogenesis in 3T3-L1 preadipocytes was investigated by measuring lipid accumulation, as well as the mRNA expression levels of various genes involved in adipocyte differentiation. Furthermore, the *in vivo* effect of orally administrated siphonaxanthin on the weight and gene expression of adipose tissue was evaluated in KK-Ay mice.

MATERIALS AND METHODS

Preparation of carotenoids.

Carotenoids, including β-carotene, zeaxanthin, lutein, fucoxanthin and violaxanthin, were prepared as previously described (44). In addition, alloxanthin, diatoxanthin, and halocynthiaxanthin were extracted from the mantle of ascidian (*Halocynthia roretzi*). Bacterioruberin was extracted from halobacteria (*Halococcus thailandensis*, JCM 13552). Loroxanthin was extracted from green alga (*Chaetomorpha crassa Kützing*), and siphonaxanthin and siphonein were extracted from green alga (*Codium fragile*, kindly donated by NOF CORPORATION, Tokyo, Japan). The extracted carotenoids were purified by HPLC (LC-6, Shimadzu, Japan). The purified carotenoids (purity $>$ 98%) were used for the *in vitro* study.

For the *in vivo* study, crude lipid was extracted from dried *C. fragile* powder with acetone. The crude lipid extract was dissolved in dichloromethane and subjected to silica gel column chromatography. The siphonaxanthin fraction was eluted with dichloromethane/acetone (6:4) and re-chromatographed using a silica gel column, followed by elution with n-hexane/acetone (6:4) to obtain crude siphonaxanthin. The siphonaxanthin-rich fraction used for the *in vivo* study contained 73% siphonaxanthin and 27% phospholipids and glyceroglycolipids.

The absorption spectrum of each carotenoid was measured using a photodiode array detector (SPD-M20A, Shimadzu) connected to the HPLC system. The mass spectra of the purified carotenoids were measured by an HPLC system connected to a mass detector (LCMC-2010EV, Shimadzu) equipped with an interface of atmospheric pressure chemical ionization. Carotenoids were stored at -80°C until use.

3T3-L1 cell culture and differentiation.

3T3-L1 preadipocytes obtained from the Health Science Research Resources Bank (Osaka, Japan) were cultured in DMEM containing 10% FBS and 1% penicillin-streptomycin in a humidified atmosphere of 95% air and 5% CO_2 at 37°C. 3T3-L1 preadipocytes were seeded in a 24-well plate and cultured as described above. Two days post-confluence (defined as day 0) the cells were differentiated with differentiation medium (MDI，DMEM containing 1.0 μmol/L dexamethasone, 0.5 mmol/L methyl-isobutyl-xanthine, 170 nmol/L insulin, 10% FBS, and 1% penicillin-streptomycin) for 2 days. The cells were then cultured in DMEM containing 10% FBS, 1% penicillin-streptomycin, and 170 nmol/L insulin, replacing the medium every other day. To study the effect of various carotenoids on the differentiation of preadipocytes to adipocytes, the carotenoids (in DMSO) were added to the MDI differentiation medium throughout the differentiation process at a concentration of 5 μmol/L. The final concentration of DMSO in the medium was adjusted to 0.1% without cytotoxicity. To test the cytotoxicity of siphonaxanthin, post-confluent 3T3-L1 preadipocytes were incubated in MDI differentiation medium with or without various concentrations of siphonaxanthin for 3 days, and the cell viability was evaluated by 3-(4,5-dimethylthiazol-2-yl)-2,5-diphenyltetrazolium bromide (MTT) assay. On day 8, intracellular lipid accumulation was analyzed by Oil red O staining as described previously (24). The stained lipid droplets within the cells were visualized using a fluorescence microscope at 20x magnification and photographed with a digital camera (Keyence BZ-9000, Japan). In order to quantify the intracellular lipid content, the stained lipid droplets were dissolved in 2-propanol and the absorbance of extracted dye was then measured at 490 nm.

Uptake of siphonaxanthin in 3T3-L1 cells.

Two days post-confluence, preadipocytes were cultured in MDI differentiation medium in the presence of siphonaxanthin for 24, 48, or 72 h. The cells were washed twice with PBS containing 10 mol/L sodium taurocholate, and siphonaxanthin was extracted three times from the cells using a mixture of dichloromethane/methanol/water (2:1:0.9, v/v/v). The dichloromethane phase was collected, dried with nitrogen, and dissolved in methanol. An aliquot of each sample was subjected to HPLC analysis, and siphonaxanthin content was quantitated from the peak area by using a standard curve obtained using purified siphonaxanthin (17).

RNA preparation and quantitative real-time RT-PCR.

Total RNA was extracted from 3T3-L1 cells or tissue by using sepasol reagent (Nacalai Tesque, Japan) according to the manufacturer's instructions, and was treated with DNase (Wako Pure Chemical Industries, Ltd., Osaka, Japan). cDNA was synthesized from 2 μg of total RNA by using SuperScript RNase II reverse transcriptase kit (Invitrogen Corp., USA) with random hexamers. For RT-PCR, cDNA was diluted and mixed with iQ SYBR green supermix (Bio-Rad Laboratories, Hercules, CA, USA) containing 1 μmol/L PCR primer (**Table 1-1**). Real-time quantitative PCR was performed by using a DNA Engine Option system (Bio-Rad Laboratories, Hercules, CA, USA). The thermal cycling conditions were 15 min at 95°C for one cycle, followed by amplification for 43 cycles with melting for 15 s at 95°C and annealing and extension for 30 s at 60°C. The expression level of each gene was normalized by using *Gapdh* as an internal control.

TABLE 1-1: GenBank accession numbers and primer sequences used in RT-PCR experiments.

Gene	sense(5'-3')	Anti-sense(5'-3')	Gene number
Acc	AAACTGCAGGTATCCCAACTCTTC	CTGTGGAACATTTAAGATACGTTTCGAAAA	NM_133360.2
Acox1	ACCTTCACTTGGGCATGTTC	TTCCAAGCCTCGAAGATGAG	NM_015729.3
Cebpa	CAGGGCAGGAGGAAGATACA	GGAAACCTGGCCTGTTGTAA	NM_007678.3
Cebpb	GCAAGAGCCGCGACAAG	GGCTCGGGCAGCTGCTT	NM_009883.3
Cpt1a	CTCCGCCTGAGCCATGAAG	CACCAGTGATGATGCCATTCT	NM_013495.2
Fabp4	GTGAAAACTTCGATGATTACATGAA	GCCTGCCACTTTCCTTGTG	NM_024406.2
Fas	CCTGGAACGAGAACACGATCT	AGACGTGTCACTCCTGGACTTG	NM_007988.3
Gapdh	*CGTCCCGTAGACAAAATGGT*	*TGCCGTGAGTGGAGTCATAC*	*NM_008084.2*
G6pd	GGTACCTACAAGTGGGTGAA	AGATGGTGAAAAGGGAAGAT	NM_008062.2
Me1	AGGGCACATTGCTTCAGTTC	TGTACAGGGCCAGTTTACCC	NM_008615.2
Pgc1a	GAAGTGGTGTAGCGACCAATC	AATGAGGGCAATCCGTCTTCA	NM_008904.2
Pgc1b	TCCTGTAAAAGCCCGGAGTAT	GCTCTGGTAGGGGCAGTGA	NM_133249.2
Pparg	GCCCTTTGGTGACTTTATGG	GGCGGTCTCCACTGAGAATA	NM_011146.3
Scd1	ACAGTCCAGGGCCAACAGT	GGCACCTTACACAGCCAGTT	NM_009127.4
Srebp1c	GGAGCCATGGATTGCACATT	GCTTCCAGAGAGGAGCCCAG	NM_011480
Ucp1	TCAGGATTGGCCTCTACGAC	TGCATTCTGACCTTCACGAC	NM_009463.3
Ucp2	TCAGAGCAGGAGGTTACAGT	TCAACCCCTTCATTACAGAC	(41)
Ucp3	GCTGAGATGGTGACCTACG	CGGGTCTTTACCACATCCAC	NM_009463.3

Western blot analysis.

Cells were washed with cold PBS twice and scraped into lysis buffer (20 mmol/L Tris-HCl, pH 8, 150 mmol/L NaCl, 1% triton-X 100, protease inhibitor mixture, and phosphatase inhibitor mixture). The cell suspensions were centrifuged at 17,800 × g at 4°C for 10 min to collect the supernatant. Protein concentration was determined by using a DC protein assay kit (Bio-Rad Laboratories, Hercules, CA, USA). Ten micrograms of protein was separated by 10% SDS-PAGE and transferred to PVDF membrane. Immunoblots were incubated with the primary antibodies for Akt (1:1000, Cell Signaling), phospho-Akt (1:2000, Cell Signaling), or β-actin (1:1000, Cell Signaling) at room temperature for 1 h, and then incubated with HRP-

conjugated anti-rabbit IgG secondary antibody, at room temperature for 1 h. Signals were visualized with the substrate, Chemi-lumi One (Nacalai Tesque, Japan) by using a FUJIFILM visualizer (LAS-3000, Fujifilm Corporation, Japan).

Mice and Diets.

All experimental animal protocols were approved by the Animal Experimentation Committee of Kyoto University for the care and use of experimental animals. Male KK-Ay/TaJcl mice (4 weeks of age) were obtained from Japan Clea Co. (Tokyo, Japan). All mice were housed individually and maintained on an alternating 12-h light/dark cycle at a temperature of 23 ± 1°C. After an acclimatization period of 1 week, the KK-Ay mice were randomly divided into two groups (n = 5), with *ad libitum* access to drinking water and the AIN-93G growth diet (45). The control group and siphonaxanthin group received daily oral treatments of 100 μL triolein or 100 μL triolein containing 1.3 mg siphonaxanthin, respectively. Body weight and food intake were monitored throughout the study. After 6 weeks of administration, mice were feed-deprived for 12 h and killed by isoflurane anesthesia. Blood was collected, and organs were rapidly removed, weighed and immediately frozen by liquid nitrogen. The WAT, BAT, liver, muscle were partly stored in RNA laterTM solution (Ambion Inc., USA) at -80°C until use for real-time RT-PCR analyses.

Biochemical Analysis.

The serum was prepared by centrifuging at 400 × g for 15 min at 4°C, and stored at -80 °C until use. Serum levels of triacylglycerol, free cholesterol, total cholesterol, HDL-cholesterol, nonesterified fatty acid (NEFA), aspartate aminotransferase (AST/GOT), alanine aminotransferase (ALT/GPT), and glucose were measured by using commercially available kits (TG E, F-Cho E, T-Cho E, HDL-C E, NEFA C, GOT·GPT C II , Glu C II; Wako Pure

Chemical Industries, Ltd., Osaka, Japan). Serum adiponectin was measured by using commercial ELISA kits (Quantikine Adiponectin/Acrp30 Immunoassay Mouse; R&D Systems). Liver triacylglycerol and total cholesterol levels were measured in the lipid fraction prepared from the liver.

Siphonaxanthin analysis in the tissues of KK-Ay mice.

Siphonaxanthin were extracted from the tissues and then subjected to a quantitative HPLC analysis (15). The lipid extracts was dissolved in dichloromethane/methanol (1:1, v/v) for HPLC analysis. For the analysis of high fat tissues (liver, brain and adipose tissue), the extracts were loaded onto a Sep-Pak Plus silica cartridges (Waters, Milford, MA, USA) to remove the triacylglycerol fraction before HPLC analysis. The peak of siphnaxanthin was further confirmed from its characteristic UV-VIS and mass spectra as described above.

Statistical analysis.

Data analyses were performed by using the statistical program SPSS 16.0 for Windows. Comparisons were made among groups of normally distributed data by using a 1-factor ANOVA followed by Tukey's post hoc analysis. Student's test was used to examine the differences between control and siphonaxanthin groups. Variance homogeneity was examined by using Levene's test. When the variances among groups were unequal, the data were transformed to logarithms before analysis by 1-factor ANOVA or were subject to a Kruskal-Wallis test. Data with unequal variances between control and siphonaxanthin groups were transformed to logarithms or were subject to a Mann-Whitney U test. For the change of siphonaxanthin content in cells, a 1-factor ANOVA with repeated measures was conducted. A repeated measures 2-factor ANOVA (time × treatment) was used to determine changes of

gene expression levels in cells. Data are represented as means ± SEMs. Statistical significance was defined as $P < 0.05$.

RESULTS

Effects of carotenoids on MDI-induced lipid accumulation in 3T3-L1 adipocytes.

The effects of 12 carotenoids on the differentiation of 3T3-L1 preadipocytes to adipocytes were firstly investigated. The cells treated with alloxanthin, bacterioruberin, β-carotene, diatoxanthin, fucoxanthin, halocynthiaxanthin loroxanthin, lutein, and siphonein showed no difference in lipid droplet accumulation in adipocytes, as compared to the differentiated control. However, the lipid droplet accumulation in cells treated with siphonaxanthin, violaxanthin and zeaxanthin was significantly decreased compared with differentiated control cells (**Fig. 1-1**). Among the 12 carotenoids, siphonaxanthin displayed the most significant inhibitory effect on adipogenesis, as lipid accumulation was decreased about 45% following 5 μmol/L treatment.

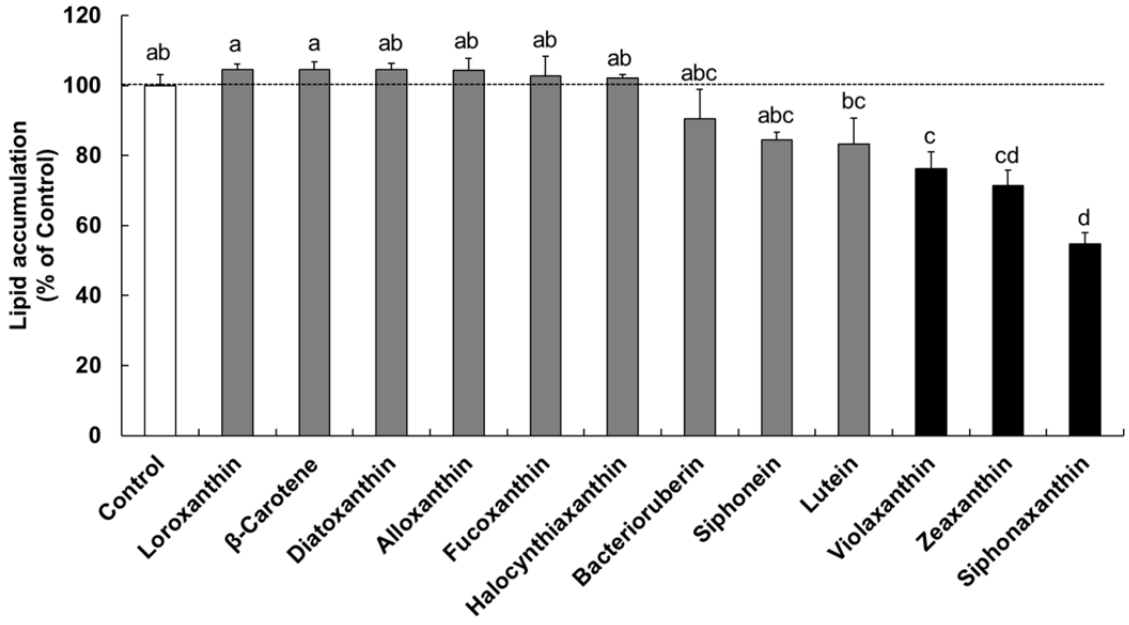

FIGURE 1-1 Effect of carotenoids on adipogenesis in 3T3-L1 cells. Lipid accumulation in adipocytes treated with MDI in the presence or absence of 5 μmol/L of various carotenoids for 8 days. Values are means ± SEMs, n = 3. Data were analyzed by Tukey's test, labeled

means without a common letter differ, $P < 0.05$. Control, differentiated adipocytes treated without carotenoids; MDI, differentiation medium.

Effects of siphonaxanthin on preadipocyte differentiation.

The treatment with siphonaxanthin at a concentration of 7.5 μmol/L for 72 h significantly decreased cell viability. In contrast, concentrations of 2.5 and 5 μmol/L, siphonaxanthin did not affect cell viability (**Fig. 1-2A**). These data indicated that the inhibitory effect of 5 μmol/L siphonaxanthin during 3T3-L1 adipocyte differentiation was not due to cytotoxicity. The concentrations with no observed cytotoxicity were used in the following studies. Morphologic analysis of intracellular lipids by Oil Red O staining showed that the number and size of single lipid droplets in siphonaxanthin-treated cells were obviously decreased compared to the control cells (**Fig. 1-2B**). Siphonaxanthin significantly reduced lipid accumulation in 3T3-L1 adipocytes in a dose-dependent manner (**Fig. 1-2C**). The siphonaxanthin content in MDI-stimulated cells after 24 h of incubation with siphonaxanthin was 4.0 ± 0.3 nmol/mg protein, whereas the content reached 6.7 ± 0.3 nmol/mg protein after 72 h of incubation (**Fig. 1-2D**).

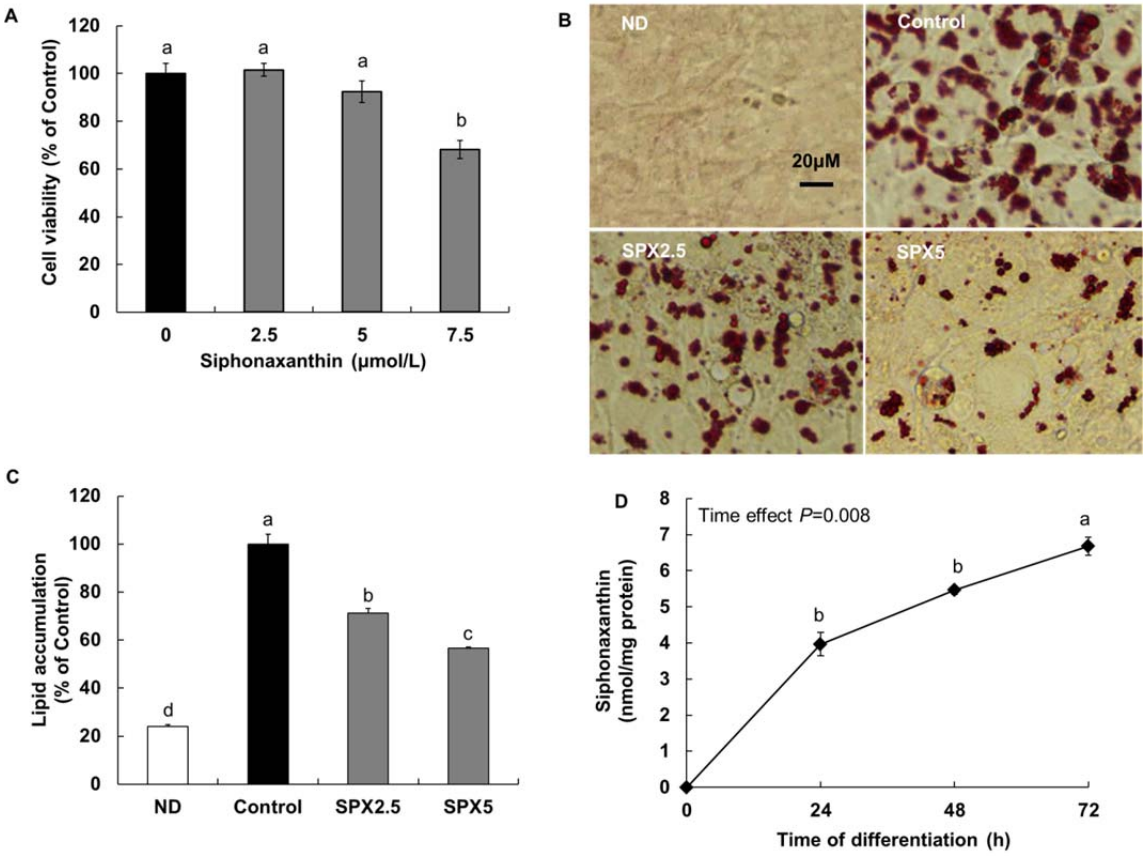

FIGURE 1-2 Effect of siphonaxanthin on adipogenesis in 3T3-L1 cells. Cell viability in differentiated cells treated with siphonaxanthin (0-7.5 μmol/L) for 72 h (A).Oil Red O staining (B) and lipid accumulation (C) in adipocyte treated with MDI in the presence or absence of 2.5 or 5 μmol/L of siphonaxanthin for 8 days. Values are means ± SEMs, n = 9 for cell viability determination, n = 6 for lipid accumulation determination Data were analyzed by Tukey's test. Changes of siphonaxanthin content in 3T3-L1 cells treated with MDI in the presence of 5 μmol/L siphonaxanthin for 24 h, 48 h and 72 h (D). Values are means ± SEMs, n = 3. Statistical significance as revealed by 1-factor ANOVA with repeated measures. Within each graph, labeled means without a common letter differ, $P < 0.05$. Control, differentiated adipocytes treated without siphonaxanthin; MDI, differentiation medium; ND, not differentiated 3T3-L1 preadipocytes; SPX2.5, 2.5 μmol/L siphonaxanthin; SPX5, 5 μmol/L siphonaxanthin.

Effects of siphonaxanthin on 3T3-L1 adipocyte differentiation at various stages during adipogenesis.

Differentiating cells were treated with 5 μmol/L siphonaxanthin for various times periods (day 0-2, 0-4, 0-6, 0-8, 2-4, 2-6, 2-8, 4-6, 4-8, and 6-8). After 8 days of differentiation, these cells were subjected to Oil red O staining. The cells treated with siphonaxanthin from day 0-8 exhibited approximately 45% inhibition of adipogenesis (**Fig. 1-3A**). Moreover, the cells treated with siphonaxanthin for day 0-6 also showed a 40% decrease in lipid accumulation, similar to those treated for 8 days (**Fig. 1-3A**). In addition, the presence of siphonaxanthin from day 0-2 and 0-4 caused a 25% decrease of lipid accumulation (**Fig. 1-3A**). However, cells treated with siphonaxanthin on days 2-4, 2-6, 4-6, 4-8, and 6-8, including intermediate and late phase of adipogenesis, did not display significantly reduced levels of lipid accumulation compared with control cells (**Fig. 1-3A**). These results indicated that the inhibitory effect of siphonaxanthin on adipogenesis occurred during the early phase. In addition, cells treated with siphonaxanthin from day 2 to 8 exhibited a significant decrease in lipid accumulation, implying a possible role for siphonaxanthin in regulating middle and later adipogenesis. Adipogenic stimuli strongly induced serine phosphorylation of Akt after 30 min, with a sustained level of phosphorylation up to 120 min; however, 5 μmol/L siphonaxanthin significantly inhibited MDI-induced Akt phosphorylation after 90 and 120 min (**Fig. 1-3B&C**).

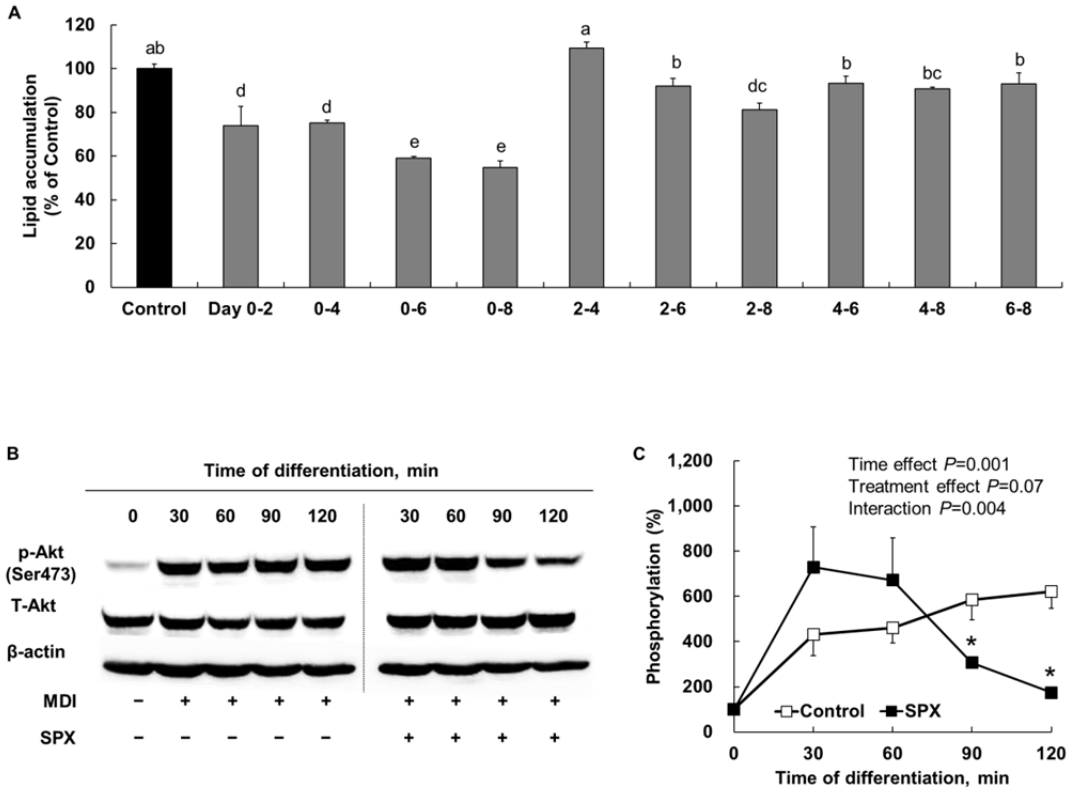

FIGURE 1-3 Effect of siphonaxanthin on 3T3-L1 adipocyte differentiation at various stages during adipogenesis (A). Post-confluent 3T3-L1 preadipocytes were differentiated with MDI medium, and 5 μmol/L siphonaxanthin was added at various stages of the adipogenesis process. At day 8 of differentiation, intracellular lipid accumulation was determined. Values are means ± SEMs, n = 3. Data were analyzed by Tukey's test. Labeled means without a common letter differ, $P < 0.05$. Akt phosphorylation in preadipocytes stimulated with MDI in the presence or absence of 5 μmol/L siphonaxanthin (B, C). Relative Akt phosphorylation (the ratio of p-Akt:T-Akt expression) expressed as percentages of undifferentiated 3T3-L1 preadipocytes are shown (C). β-Actin was used as references. Values are means ± SEMs, n = 3. Statistical significance as revealed by a repeated measures 2-factor ANOVA (time × treatment), followed by Student's t test. *Different from control at each time, $P < 0.05$. Akt, protein kinase B; Control, differentiated adipocytes treated without siphonaxanthin; MDI, differentiation medium; p-, phosphorylated; SPX, siphonaxanthin; T-, total.

Effects of siphonaxanthin on adipogenic transcription factors and target genes.

To identify the molecular mechanisms underlying the inhibitory effect of siphonaxanthin on adipocyte differentiation, the expression of key adipogenic transcription factors and target genes was analyzed at various time points during 3T3-L1 adipocyte differentiation. The expression of CCAAT/enhancer binding protein beta (*Cebpb*) was increased following MDI stimulation up to 4 h, at which point it was then decreased (**Fig. 1-4A**). Further, *Cebpb* expression was not changed following siphonaxanthin treatment. Sterol regulatory element binding protein (*Srebp1c*) is an insulin-regulated gene, and its expression was not altered in MDI-stimulated 3T3-L1 cells in the presence of siphonaxanthin (**Fig. 1-4B**). The expression of *Cebpa* was increased 1.8- to 4-fold in cells during differentiation process, and the expression of *Pparg* was also increased 1.6- to 2.6-fold compared to non-differentiated 3T3-L1 preadipocytes; however, their expression was significantly suppressed in siphonaxanthin-treated cells (**Fig. 1-4C&D**). Fatty acid binding protein 4 (*Fabp4*) (46) mRNA expression was increased more than 100-fold in cells undergoing adipogenesis; however, the expression of *Fabp4* was almost completely inhibited by treatment with siphonaxanthin (**Fig. 1-4E**). Stearoyl CoA desaturase 1 (*Scd1*) (47) mRNA expression was increased more than 8-fold during adipogenesis, but was significantly inhibited following siphonaxanthin treatment (**Fig. 1-4F**). Importantly, siphonaxanthin almost lowered the mRNA levels of these genes to the levels observed in undifferentiated cells after 6 or 8 days of adipocyte differentiation.

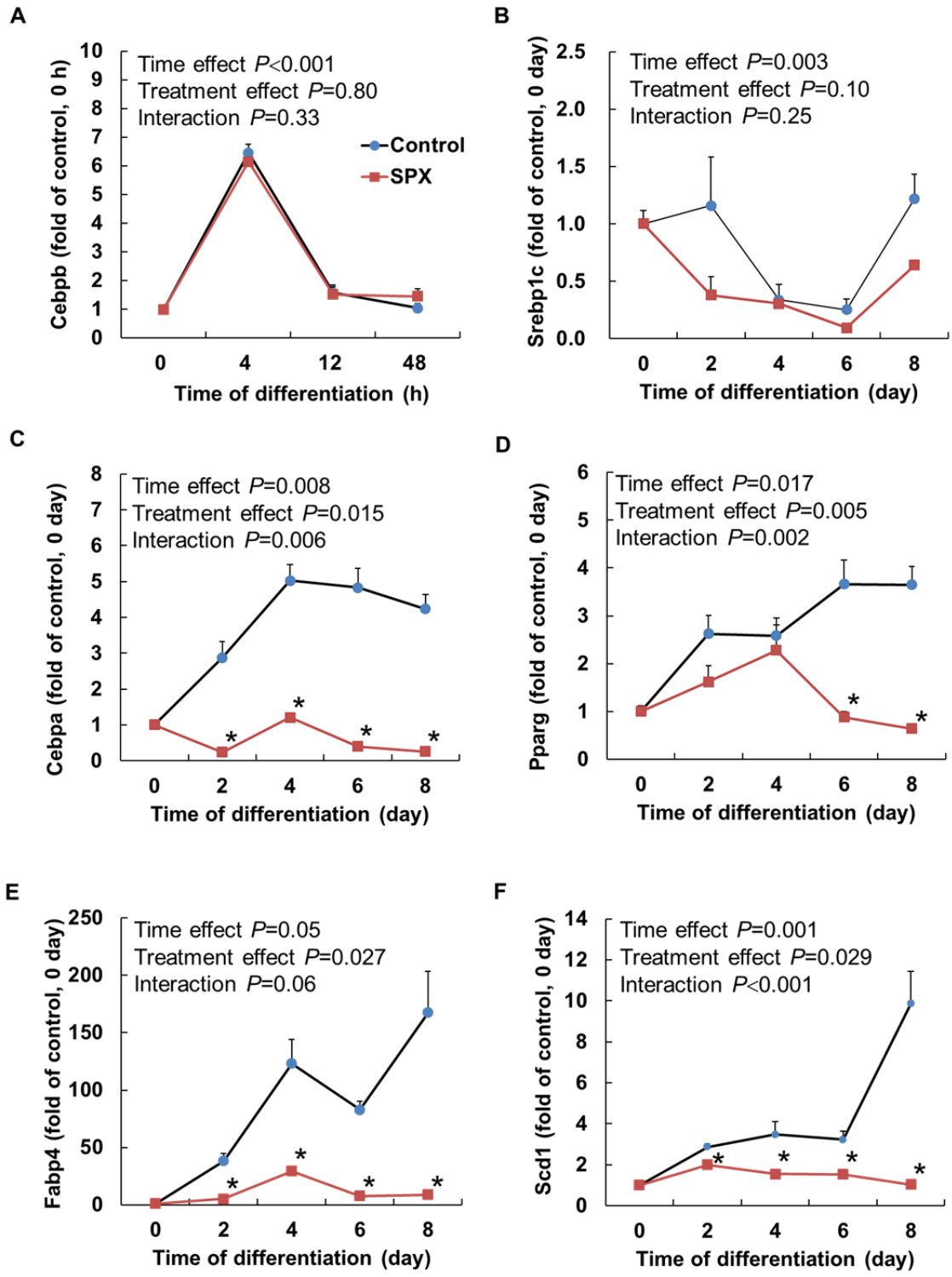

FIGURE 1-4 Effects of siphonaxanthin on *Cebpb* (A), *Srebp1c* (B), *Cebpa* (C), *Pparg* (D), *Fabp4* (E) and *Scd1* (F) mRNA levels of genes involved in adipogenesis. Preadipocytes were differentiated with MDI in the presence or absence of 5 μmol/L siphonaxanthin, and mRNA

levels were determined at various time points. Values were normalized to *Gapdh.* Values are means ± SEMs, $n = 3$. Statistical significance as revealed by a repeated measures 2-factor ANOVA (time × treatment), followed by Student's t test. *Different from control at each time, $P < 0.05$. C*ebpa*, CCAAT/enhancer binding protein alpha; *Cebpb*, CCAAT/enhancer binding protein beta; Control, differentiated adipocytes treated without siphonaxanthin; *Fabp4*, fatty acid binding protein 4; *Pparg*, PPAR gamma; *Scd1*, stearoyl CoA desaturase 1; SPX, siphonaxanthin; *Srebp1c*, sterol regulatory element binding protein 1c.

Effects of orally administrated siphonaxanthin on body weight, adiposity, serum, and liver parameters in KK-Ay mice.

Based on above-mentioned *in vitro* observations, an *in vivo* experiment using KK-Ay mice was performed. Siphonaxanthin dissolved in triolein was orally administered to each mouse daily for 6 weeks. There was no significant difference in the food intake, body weight gain, and liver weight between the control and siphonaxanthin groups (**Table 1-2**). Siphonaxanthin significantly reduced the weight of total white adipose tissue and mesenteric adipose tissue compared with the control group, although the weights of the epididymal, perirenal, and interscapular adipose tissue were not altered (**Table 1-2**). The serum levels of triacylglycerol, free cholesterol, total cholesterol, HDL-cholesterol, NEFA, glucose, and adiponectin were not significantly different between the control group and the siphonaxanthin group. Furthermore, serum AST and ALT levels of the siphonaxanthin group did not differ from those of the control group (**Table 1-2**), indicating that siphonaxanthin treatment at this dose did not cause damage to the liver. The levels of triacylglycerol and total cholesterol in the liver did not differ between treatments (**Table 1-2**).

TABLE 1-2 Effect of siphonaxanthin on body weight, adipose tissue mass, plasma parameters and lipid metabolism in KK-Ay mice [1]

	Control	Siphonaxanthin
Body weight gain (g/6 week)	13.6 ± 0.7	13.8 ± 1.0
Food intake (g/day)	4.34 ± 0.04	4.35 ± 0.05
Liver weight (g)	4.20 ± 0.25	4.04 ± 0.19
BAT (g/100 g body weight)	0.81 ± 0.05	0.78 ± 0.07
Total WAT (g/100 g body weight)	10.3 ± 0.1	8.99 ± 0.6*
Mesenteric WAT (g/100 g body weight)	3.08 ± 0.12	2.22 ± 0.05*
Epididymal WAT (g/100 g body weight)	4.57 ± 0.12	4.51 ± 0.21
Perirenal WAT (g/100 g body weight)	2.69 ± 0.06	2.26 ± 0.36
Plasma triacylglycerol (mg/dL)	139 ± 14.9	123 ± 22.8
Plasma free cholesterol (mg/dL)	31.1 ± 1.9	26.2 ± 2.2
Plasma total cholesterol (mg/dL)	126 ± 7.2	105 ± 9.1
HDL-cholesterol (mg/dL)	83.1 ± 4.7	67.3 ± 6.6
NEFA (mEq/L)	0.65 ± 0.04	0.67 ± 0.05
Glucose (mg/dL)	268 ± 36.1	193 ± 36.4
AST (U/L)	32.97±1.85	33.23±5.00
ALT (U/L)	8.33±0.37	8.89±0.58
Adiponectin (μg/mL)	4.66 ± 0.20	4.18 ± 0.23
Liver triacylglycerol (mg/g liver)	54.2 ± 12.9	40.0 ± 2.6
Liver cholesterol (mg/g liver)	7.61 ± 0.44	9.45 ± 1.20

[1] Values are means ± SEMs, $n = 5$. Data were analyzed by Student's t test. *Different from control, $P < 0.05$. ALT, alanine aminotransferase; AST, aspartate aminotransferase; BAT, brown adipose tissue; Control, mice treated without siphonaxanthin; NEFA, nonesterified fatty acid; WAT, white adipose tissue.

Effects of siphonaxanthin on the expression of mRNA related to lipid metabolism in KK-Ay mice.

The effects of siphonaxanthin on the expression of adipogenic factors and lipid-regulating enzymes in the tissues of KK-Ay mice, including the liver, mesenteric adipose tissue, and skeletal muscle, were investigated by using real time RT-PCR analysis. Siphonaxanthin-treated mice tended to have a lower expression of *Cebpa* ($P = 0.08$) and *Pparg* ($P = 0.06$) in the mesenteric adipose tissue compared with control mice, although this was not significant (**Fig. 1-5A**). Siphonaxanthin significantly downregulated the mRNA expression of *Scd1* and glucose-6-phosphate dehydrogenase (*G6pd*) in mesenteric adipose tissue compared with the control group, but did not affect the mRNA expression of *Srebp1c*, *Acc*, and malic enzyme 1 (*Me1*) (**Fig. 1-5A**). In contrast to the lipogenic genes analyzed, the mRNA expression of the β-oxidation related gene carnitine palmitoyltransferase 1a (*Cpt1a*) and the energy expenditure-related gene PPAR gamma coactivator 1 beta (*Pgc1b*) was upregulated in the siphonaxanthin group, whereas the mRNA expression of PPAR gamma coactivator 1 alpha (*Pgc1a*) and acyl-CoA oxidase 1 (*Acox1*) was not altered (**Fig. 1-5B**). In the liver, expression levels of fatty acid synthesis-related genes, including *Srebp1c*, fatty acid synthase (*Fas*), *Scd1*, and acetyl-CoA carboxylase (*Acc*) were measured; however, no significant difference was observed between treatments (**Fig. 1-5C**). Siphonaxanthin also significantly increased the mRNA expression of uncoupling protein 3 (*Ucp3*) in skeletal muscle (**Fig. 1-5D**). Siphonaxanthin did not change the mRNA expression of *Ucps* in brown adipose tissue (BAT) (**Fig. 1-5E**).

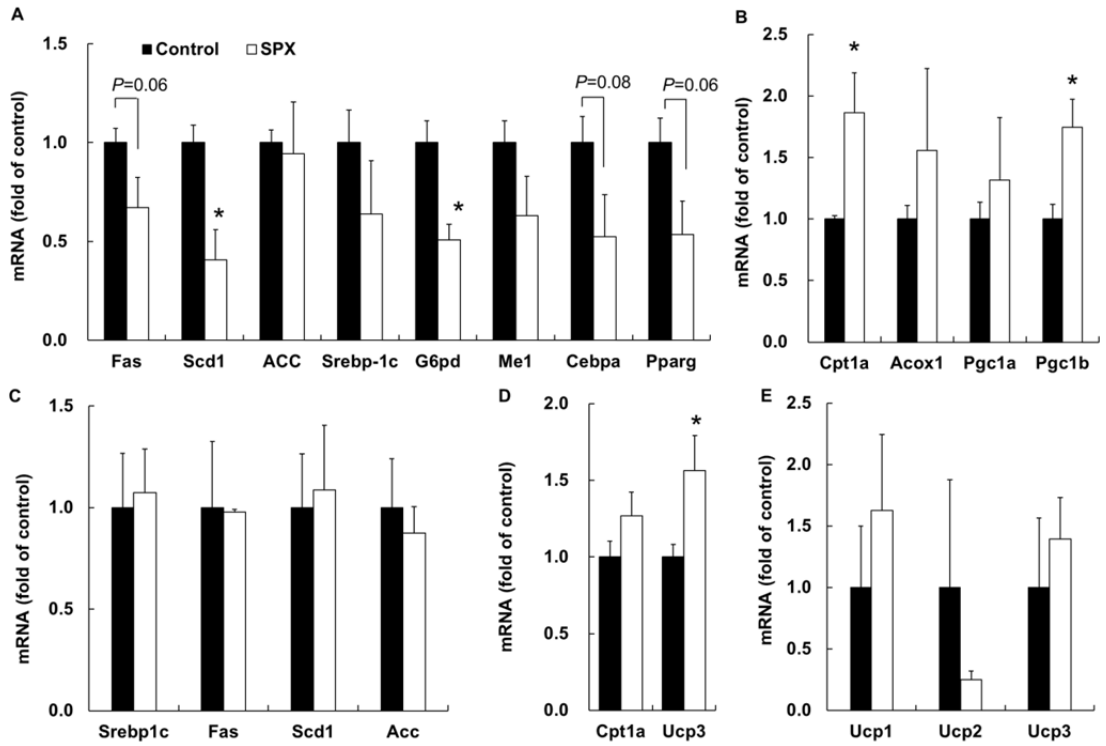

FIGURE 1-5 Effects of siphonaxanthin on the mRNA expression level of genes involved in lipid metabolism in mesenteric adipose tissue and skeletal muscle. KK-Ay mice were treated with siphonaxanthin for 6 weeks. Lipogenesis markers (*Fas*, *Scd1*, *Acc*, *Srebp1c*, *G6pd*, *Me1*, *Cebpa* and *Pparg*) mRNA expression in the mesenteric adipose tissue (A). Fatty acid oxidation markers (*Cpt1a*, *Acox1*, *Pgc1a* and *Pgc1b*) mRNA expression in the mesenteric adipose tissue (B). mRNA expression of *Srebp1c*, *Fas*, *Scd1* and *Acc* in the liver (C). mRNA expression of *Cpt1a* and *Ucp3* in the skeletal muscle (D). mRNA expression of *Ucp1, Ucp2, and Ucp3* in the brown adipose tissue (E). Values are means ± SEMs, $n = 5$. Data were analyzed by Student's t test. *Different from control, $P < 0.05$. *Acc*, acetyl-CoA carboxylase; *Acox1*, acyl-CoA oxidase 1; *Cebpa,* CCAAT/enhancer binding protein alpha; Control, mice treated without siphonaxanthin; *Cpt1a*, carnitine palmitoyltransferase 1a; *Fas*, fatty acid synthase; *G6pd*, glucose-6-phosphate dehydrogenase; *Me1*, malic enzyme 1; *Pgc1a* peroxisome proliferative activated receptor gamma coactivator 1 alpha; *Pgc1b* peroxisome

proliferative activated receptor gamma coactivator 1 beta; *Pparg*, PPAR gamma; *Scd1*, stearoyl CoA desaturase 1; SPX, siphonaxanthin; *Srebp1c*, sterol regulatory element binding protein 1c; *Ucp3*, uncoupling protein 3.

Accumulation of siphonaxanthin in the tissues of KK-Ay mice.

Siphonaxanthin was detected in each tissue of KK-Ay mice after oral administration for 6 weeks by HPLC analysis, except for bladder, brain and small intestine (**Fig. 1-6**). Siphonaxanthin were highly accumulated in WAT and digestion-associated tissues (pancreas, large intestine, and stomach) (F**ig. 1-6**). Notably, the accumulation in mesenteric WAT was the highest among all tissues and was approximately 2- and 3-fold of that in the epididymal and perirenal WAT, respectively (**Fig. 1-6**). The siphonaxanthin accumulation in others tissues (heart, liver, testis muscle, kidney, lung and spleen) was less than10% of the amount in mesenteric WAT (**Fig. 1-6**). In addition, some unidentified peaks near the peak of siphonaxanthin appeared in the chromatograms of the tissues in which siphonaxanthin was detected. These peaks might be oxidation metabolites of siphonaxanthin.

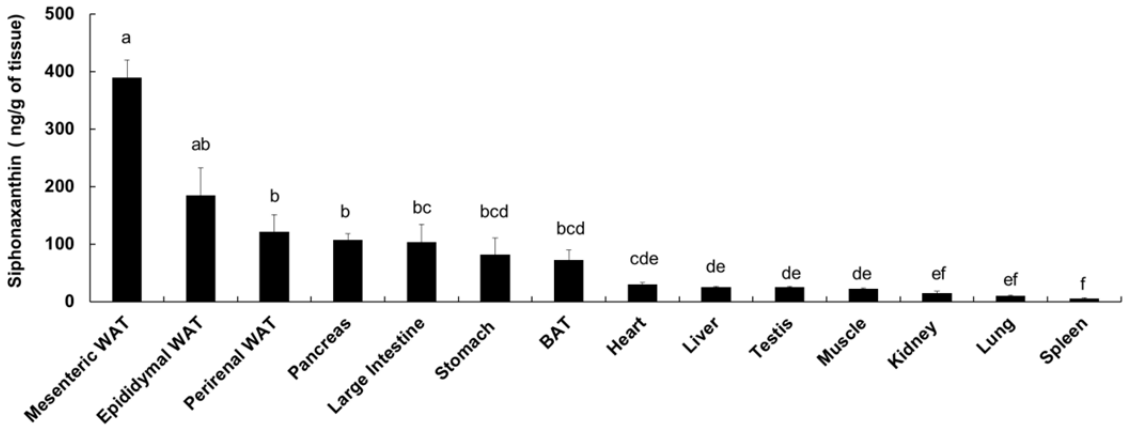

FIGURE 1-6 Accumulation of siphonaxanthin in the tissues of KK-Ay mice treated with

siphonaxanthin for 6 weeks. Values are means ± SEMs, $n = 5$. Data were analyzed by Tukey's test. Labeled means without a common letter differ, $P < 0.05$. BAT, brown adipose tissue; WAT, white adipose tissue.

DISCUSSION

In this chapter, the effect of siphonaxanthin on adipocyte differentiation in 3T3-L1 cells and obesity in a diabetic/obese KK-Ay mice model was examined. It is observed that siphonaxanthin significantly suppressed 3T3-L1 adipocyte differentiation via the downregulation of the transcription factors *Cebpa* and *Pparg*, which strictly govern adipocyte differentiation. Further, the development of total and mesenteric adipose tissue was significantly decreased in siphonaxanthin-treated KK-Ay mice.

Firstly, 12 carotenoids were screened to evaluate their anti-adipogenesis activity and identified siphonaxanthin as a compound that potently inhibits adipogenesis. It is assumed that the anti-adipogenic activity of siphonaxanthin is likely associated with its unique structure. Treatment with carotenoids without extra functional groups, including keto groups and hydroxyl groups, on the carbon skeleton (β-carotene) did not result in a significant inhibition of lipid accumulation in adipocytes. Maeda et al. have been reported that fucoxanthin at a higher concentration (10-25 μmol/L) can decrease lipid accumulation in 3T3-L1 cells (24). Although both fucoxanthin and siphonaxanthin are keto-carotenoids, fucoxanthin has an epoxide group and an allenic bond in its molecular structure, while siphonaxanthin has a hydroxyl group at C-19. An analog of siphonaxanthin, loroxanthin, which has no keto group, did not inhibit adipocyte differentiation. Likewise, siphonein, which is 12:1-esterified at the C-19 hydroxyl group of siphonaxanthin, had no significant inhibitory effect on adipocyte differentiation. It is assumed that the presence of both the keto group and the hydroxyl group may be important for the inhibitory effect of siphonaxanthin on adipocyte differentiation.

The anti-adipogenic effect of siphonaxanthin is likely due its ability to modulate cellular events during the early stage of adipocyte differentiation. The insulin-dependent

phosphatidylinositol-3 kinase (PI3K)-Akt signaling pathway is thought to be important for the initiation of molecular events in adipogenesis. Previous work demonstrated that Akt activated in response to insulin plays a critical role in the development and maintenance of proper adipose tissue (48). The phosphorylation of Akt occurs within the first several hours after insulin stimulation, and it is shown to be necessary for 3T3-L1 adipocyte differentiation (49, 50). The expression and function of PPARG and CEBPs are regulated by transcription factors activated by the Akt signaling cascade, including GATA2 and cyclic AMP response element-binding protein (33). The present observation is in accordance with a previous report in which siphonaxanthin inhibited the phosphorylation of Akt at the low concentrations (0.1 and 0.5 μmol/L) in vascular endothelial cells (14). In this study, it is speculated that siphonaxanthin may have no effect on the upstream components of the Akt signaling cascade, including the insulin receptor, insulin receptor substrate, and PI3K. Further studies are needed to determine how intracellular siphonaxanthin modulates the insulin signaling pathway in the early stage of adipogenesis.

During adipogenesis, transient activation of CEBPB expression and its phosphorylation by insulin-activated MAP kinase and glycogen synthase kinase 3β are thought to be involved in the initiation of mitotic clonal expansion and the induction of pleiotropic transcription factors, such as CEBPA and PPARG (51-53). In this study, the results showed that *Cebpb* gene expression was not influenced by siphonaxanthin treatment. Similar results have also been described in 3T3-L1 cells treated with other anti-adipogenic substances, such as β-cryptoxanthin, curcumin, and neoxanthin (54-56). Moreover, it is reported that genistein and dehydrodiconiferyl alcohol did not affect CEBPB protein levels, although they inhibited the activity of CEBPB, such as its phosphorylation, DNA-binding, and centromeric localization (57, 58). Interestingly, siphonaxanthin reduced the mRNA levels of *Cebpa* and *Pparg*, which is likely a consequence of CEBPB function in the early phase of adipogenesis. Therefore, it is

hypothesized that siphonaxanthin may interfere with the activity or the downstream target of CEBPB during adipogenesis.

Maeda *et al.* reported that dietary fucoxanthin (0.2% of diet) significantly reduced the weight of abdominal white adipose tissue and blood glucose in KK-Ay mice fed a high fat diet, but weight was not altered with less than 0.1% fucoxanthin (59). The observations in this chapter implied that siphonaxanthin was more effective in inhibiting adipogenesis than fucoxanthin in 3T3-L1 cells, and that the weight of the total and mesenteric white adipose tissue in KK-Ay mice fed a normal diet were significantly reduced by oral administration of siphonaxanthin at a low dosage (equal to 0.03% dietary siphonaxanthin). Since the expression levels of *Cebpa* and *Pparg* tended to be lowered in mice treated with siphonaxanthin, similar to the results in the cultured cell model, the reduction of adipose tissue in siphonaxanthin-treated mice may be partly due to the inhibition of adipocyte differentiation. Another possibility is that lipid accumulation was suppressed in pre-existing adipocytes via the reduction of lipid synthesis and the enhancement of fatty acid oxidation. SREBP1c and its target genes *Scd1*, *Fas*, and *Acc* are involved in adipogenesis and lipogenesis, and they are thought to have an important role in regulating fatty acid synthesis (60). The results in this study indicated that siphonaxanthin significantly downregulated the expression of *Scd1* and *G6pd* in mesenteric adipose tissue, and had a tendency to lower the expression of *Fas*. In addition, ACOX1 and CPT1A are the key enzymes involved in fatty acid oxidation systems, and the PGC1 family have emerged as key players in the control of mitochondrial biogenesis and oxidative metabolism in adipose tissue (61, 62)**.** The expression of *Cpt1a* and *Pgc1b* in mesenteric adipose tissue was significantly upregulated by siphonaxanthin treatment in KK-Ay mice. UCPs in brown adipose tissue are known to have a major role in whole body thermogenesis, and the downregulation of their expression contributes to rapid weight gain (63). In particular, UCP3, which is predominantly expressed in skeletal muscle, supports a

role in energy balance and lipid metabolism (64). Siphonaxanthin did not modulate the expression of *Ucp*s in BAT; however, it significantly enhanced the expression of *Ucp3* in skeletal muscle. These data indicated that the anti-obesity effect of siphonaxanthin observed in this study may be caused by the combination of reduction in lipid synthesis and enhancement in fatty acid oxidation.

It was reported that *Pparg*-deficient models and *Pparg* antagonists induce insulin resistance, which was caused by a lack of adequate adipose tissue mass contributing to impaired glucose metabolism and reduction of leptin secretion (65). The anti-adipogenic effect of siphonaxanthin would be due to suppression of *Pparg* expression, so it is considered whether siphonaxanthin lead to other deleterious effects, such as a reduction in insulin sensitivity *in vivo*. In the present results, however, plasma glucose level tended to decrease by the administration of siphonxanthin. Even though further studies are needed, anti-adipogenic effect of siphonaxanthin with fewer side effects might be desirable for the prevention of obesity.

In this study, glucose, triacylglycerol and cholesterol levels in plasma of siphonaxanthin-treated mice were 72, 89 and 84% of control mice, respectively, but not significant as expected. Compared to the results of cultured cell study, the modest response of siphonaxanthin *in vivo* may be due to bioavailability, metabolic fate and tissue distribution in mice of siphonaxanthin following oral administration. There had been no information about the distribution and accumulation of siphonaxanthin and its metabolites after oral ingestion. In the current study, the selective accumulation of siphonaxanthin in WAT, especially mesenteric WAT, was found for the first time. This observation may partly explain the specific effect to mesenteric WAT by oral administration of siphonaxanthin. In addition, some unknown metabolites of siphonaxantin were detected in each tissue including the mesenteric

WAT. The biological effect of these metabolites on the adipose tissue should be important for understanding of the findings in this chapter. In the present study, KK-Ay mice which spontaneously become obese, hyperinsulinaemia and hyperglycemia caused by a very strong genetic tendency toward obesity was used as an animal model. In addition, the dose of siphonaxanthin was relatively low compared to the effective dose of fucoxanhin in previous reports (39, 41, 59). It should be worthwhile therefore to evaluate the dose response of siphonaxanthin *in vivo* using other models, such as high-fat diet induced obesity model.

The results in this chapter indicate that siphonaxanthin may be a useful dietary supplement for the regulation of lipid accumulation in adipose tissue. The findings suggest for the first time such a role for siphonaxanthin in adipogenesis, although further studies are required to understand its mechanism and metabolism.

INTRODUCTION

Carotenoids are structurally and functionally a very diverse group of natural pigments of the polyene type. Carotenoids with structure of conjugated double bonds are known to be very potent natural antioxidants, due to their ability to physically and chemically quench singlet oxygen, and scavenge other reactive oxygen species (66, 67). The antioxidant potential of carotenoids is of particular significance to human health, owing to its ameliorating effects on the oxidative stress, which is an essential contributor to the pathogenic processes of many diseases (68, 69). Several epidemiological studies found that dietary carotenoids are associated with reduced risk of disease, particularly certain cancers and eye disease (20, 70). Xanthophylls are carotenoids containing at least 1 hydroxyl group, such as lutein and zeaxanthin, which are the specific carotenoids found in human retina and lens and may serve a unique role in the protection against eye disease (20).

Since a number of factors might influence the bioavailability, absorption, transport, metabolism or accumulation of dietary carotenoids, the exact mechanisms for their biological function *in vivo* are still far from being fully elucidated. Current research is focused on not only exploring the potential of carotenoids in human health but also elucidating important aspects of carotenoids digestion, absorption and bio metabolism. The degree of food matrix disruption and the other dietary components could affect *in vivo* action of carotenoids (71). For instance, food processing and the amount of fat was shown to improve carotenoid bioavailability, while dietary fibers have been known to lower the intestinal absorption of carotenoid from plants or fruits (72). Other factors, individual differences including genetic factors, gender, age, and nutritional status, also affect carotenoids bioavailability. It is suggested that the absorption of most carotenoids is involved in several steps, including release of carotenoid from food matrix by heat, mechanical and enzymatic treatments during

food processing, dispersion into lipid emulsion particles in the stomach, incorporation into mixed micelles by the action of bile salt, biliary phospholipids and dietary lipids, uptake by intestinal cells, package into chylomicrons, and secretion into the lymphatic system (68, 72, 73). After the hydrolysis of lipids in chylomicrons by lipoprotein lipase, the carotenoids were released, transported in the blood, and further distributed in tissues (74).

Polar xanthophylls, such as astaxanthin, fucoxanthin, and siphonaxanthin, which are generally present in the marine organism, have been shown to possess beneficial bioactivity in animal models or human. Siphonaxanthin is a marine carotenoid and one of the oxidative metabolites of lutein. Its structure contains a structure similar to lutein except for one keto group located at C-8 and an extra hydroxyl group at C-19. This xanthophyll is special carotenoid found in green algae, such as *Caulerpa lentillifera*, *Codium fragile*, *Codium cylindricum*. In the previous study, siphonaxanthin potently inhibited angiogenic effect and induced apoptosis (14, 15). In the chapter 1, the inhibitory effects of siphonaxanthin on lipid accumulation in the 3T3-L1 cell line and KK-Ay mice were found. The bioavailability and biotransformation of siphonaxanthin concern the use of siphonaxanthin in dietary intervention for its bioactivities *in vivo*.

The human colonic adenocarcinoma (Caco-2) cell line is a well characterized model system imitating the function and structure of intestinal enterocytes (75). When cultured under specific conditions, the cells spontaneously differentiate into phenotype with some characteristics of the enterocyte, including expression of tight junctions, microvilli and a number of enzymes and transporters associated with digestion and absorption. The differentiated cell monolayers morphologically and functionally resemble the enterocytes lining the small intestine (76, 77). Thus the cell line has been widely used as an *in vitro* model to study and predict the *in vivo* intestinal absorption and transport of compounds at an early

stage of the development of drug or supplement (78).

In this chapter, the absorption and biotransformation of siphonaxanthin were evaluated using the intestinal Caco-2 cells. Furthermore, the tissue distribution and metabolic transformation of siphonaxanthin were evaluated in ICR mice.

MATERIALS AND METHODS

Preparation of siphonaxanthin

The purification of siphonaxanthin from green alga (*Codium cylindricum*) were performed as described in the chapter1.

Cell culture

Caco-2 cells obtained from RIKEN Gene Bank (Tokyo, Japan) were cultured in DMEM containing 10% FBS, 1% penicillin-streptomycin (PS) and 1% mem non-essential amino acids in a humidified atmosphere of 95% air and 5% CO_2 at 37°C. For differentiation, cells were seeded in 12-well plates at 2.0×10^5 cells/well in 1mL DMEM medium described above and allowed to differentiate until day 22 from seeding. Medium was regularly changed three times a week. Experiments were performed at day 22 post-seeding on 12-well plates.

Treatment of Caco-2 cells with micellar siphonaxanthin

Siphonaxanthin solubilized in micelles was added to medium for treatment, and the micelle formation was performed as previously described (79). Briefly, the sodium taurocholate, monoolein, oleic acid, lysophosphatidylcholine and siphonaxanthin dissolved in dichloromethane or methanol were mixed with a vortex mixer, and the organic solvent was evaporated by nitrogen gas. The residue was then dissolved in serum-free DMEM. The final concentration of each component in the medium was adjusted to as follows: 2 mmol/L sodium taurocholate, 100 μmol/L monoolein, 33.3 μmol/L oleic acid, 50 μmol/L lysophosphatidylcholine and 1.0 μmol/L siphonaxathin. The resultant solution should be optically clear. This medium was sterilized by 0.22 μm filter before being supplemented to culture cell. The concentration of micellar carotenoid was determined to be 1.0 ± 0.05 μmol/L

by HPLC before being used in the following experiment.

The cell monolayers on 12-well plates were rinsed with serum-free medium, and then incubated in 1mL of the medium containing micellar siphonaxanthin. After incubation for 0, 1, 3, 6, 24 h, the medium was collected and the cells were washed twice with ice-cold phosphate buffered saline (PBS) containing 10 mmol/L sodium taurocholate to remove surface-bonded carotenoids, followed by an additional washing with PBS. The cells were scraped into PBS and then centrifuged at 1000 g at 4°C for 5 min. The cell pellets were resuspended in 0.5 mL PBS and homogenized with a sonicator (Qsonica Q55). To extract the siphonaxanthin, the 0.4 mL cell homogenate was mixed with 1.5 mL of dichloromethane/methanol (1:2, v/v), vigorously vortexed. Then, 0.75 mL of hexane was added to the mixture, followed by strong agitation and centrifugation at 1690 g at 4°C for 10 min. The upper organic phase was transferred to a new test tube, and the sample was extracted again with adding 0.5 mL of dichloromethane, and then 0.75 mL of hexane. Such an extraction was repeated three times. All the organic phase were pooled together and evaporated gently under a nitrogen stream. The residue was dissolved in methanol and subjected HPLC analysis as described below. The concentration of siphonaxanthin in medium was also analyzed. An aliquot of medium was mixed with 4-fold methanol and subjected to HPLC analysis.

Animal studies

All animal experiments were performed according to the guidelines of the Animal Experimentation Committee of Kyoto University for the care and use of experimental animals. Male ICR mice (7 weeks of age) were purchased from Japan Shimizu Laboratory Supplies Co., Ltd. (Kyoto, Japan). All mice were housed individually and maintained on an alternating 12-h light/dark cycle at a temperature of 23±1°C and free access to drinking water

and chow (Oriental Yeast Co., Ltd., Tokyo, Japan). After an acclimatization period of 1 week, the mice were randomly divided into control and siphonaxanthin groups (n = 4 per group). The control group of mice was fed an AIN-93G diet. The siphonaxanthin group of mice was fed the AIN-93G diet with siphonaxanthin supplementation, 65.79 nmol/g of diet (0.004%). The total food intake and the body weight were recorded every day. After dietary treatments for 16 days, the mice were anesthetized under isoflurane. The blood was collected from the caudal vena cava. The plasma was prepared by centrifuging at 400 g for 15 min at 4°C. The tissues were rapidly removed, weighed and immediately frozen by liquid nitrogen, and then stored at -80°C until use.

Carotenoids were then extracted from the plasma and tissues. Briefly, the aliquots of tissue sample (0.2 g) were homogenized in a 9-fold volume of 0.9% NaCl saline with a homogenizer dispenser (T10 basic ULTRA-TURRAX, IKA). Plasma samples were diluted with 3-fold volume of Mill-Q water. The resultant tissues homogenates (0.9 mL) or diluent plasma samples (0.9 mL) were mixed with 3 mL of dichloromethane/methanol (2:1, v/v) to extract carotenoid. The samples were extracted three times, and the dichloromethane layer was collected after centrifugation at 1690 g at 4°C for 10 min. After evaporation under nitrogen, the residue was resuspended in 20 μL dichloromethane and methanol (1:1, v/v) for HPLC analysis.

HPLC analysis

HPLC analysis was carried out with a Prominence LC system (Shimadzu, Kyoto, Japan), connected to a photodiode array detector (SPD-M20A, Shimadzu) followed by an ion trap-time of flight mass spectrometer (LCMS-IT-TOF, Shimadzu) equipped with an atmospheric pressure chemical ionization (APCI) source or electrospray ionization (ESI) source. Siphonaxanthin was separated on a TSK gel ODS-80Ts QA column (2.0 × 250 mm, 5μm,

Tosoh, Japan). The binary gradient mobile phases were methanol/water (72:15, v/v) containing 0.1% ammonium acetate as mobile phase A and ethyl acetate/methanol (30:70, v/v) containing 0.1% ammonium acetate as mobile phase B. The column was eluted at a flow rate of 0.2 mL/min using the following gradients: 0-30 min, 0% B; 30-45 min, 0-100% B; 45-60 min, 100% B; 60-65 min, 100-0% B; 65-70min, 0% B. Siphonaxanthin was detected at 445 nm. The APCI source was heated at 200°C and the probe was kept at 400°C. Nitrogen was used as sheath gas at 2.0 L/min and drying gas was used at 25 kPa. Mass spectra were recorded in positive ion mode. For ESI source, sheath gas was set at 1.5L/min, and drying gas was used at 120 kPa. A spray voltage of 4.5 kV was used for the positive ionization. The peak identities for siphonaxanthin and its metabolites were further confirmed from their characteristic UV-vis spectra and their positive ions. Siphonaxanthin was quantified from their peak area at 450 nm by use of a standard curve with purified siphonaxanthin. Due to the unavailability of standards, siphonaxanthin metabolites were estimated from the siphonaxanthin standard curve (80).

Statistical analysis

Data analyses were performed by using the statistical program SPSS 16.0 for Windows. Change of concentration of siphonaxanthin in Caco-2 cells was analyzed by 1-factor ANOVA with repeated measures. Data are represented as means ± SEMs. Statistical significance was defined as $P < 0.05$.

RESULTS

Uptake siphonaxanthin by Caco-2 cells

Firstly, the uptake of siphonaxanthin was evaluated in Caco-2 cells as a model for intestinal epithelial absorption. Caco-2 cells were incubated with 1 nmol/well siphonaxanthin solubilized micelles for 1, 3, 6 and 24 h. The concentration of siphonaxanthin in cells, medium and the total culture (cells and medium) was quantified (**Fig. 2-1**). The cellular concentration of siphonaxanthin was rapidly and linearly increased until 3 h after incubation, and then gradually increased until 24 h. The concentration of siphonaxanthin in medium decreased accordingly as increased the incubation time (**Fig. 2-1**). The similar trend was also observed from the culture (**Fig. 2-1**).

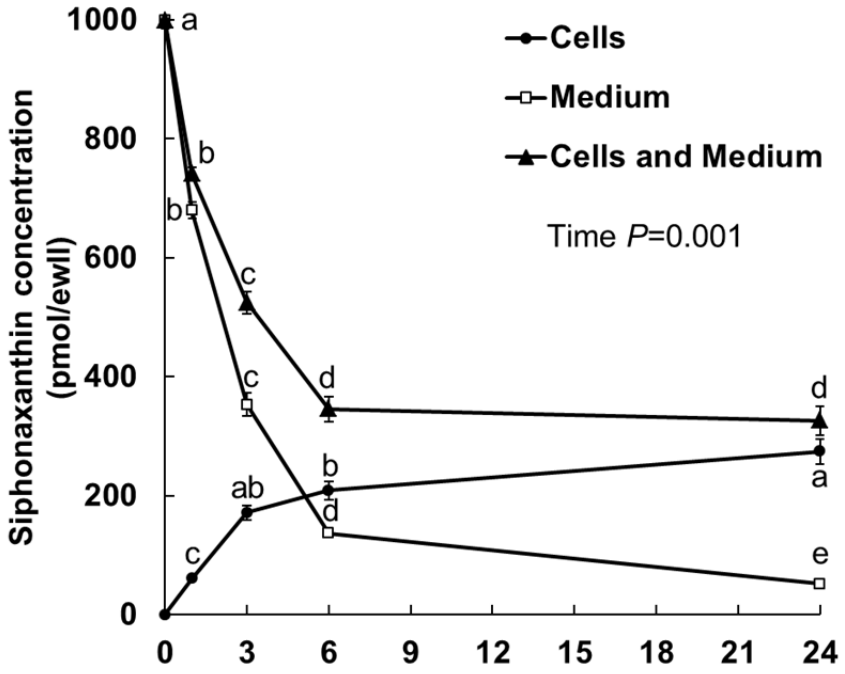

FIGURE 2-1 Changes of siphonaxanthin concentration in Caco-2 cells and medium. Differentiated Caco-2 cells were treated with mixed micelles containing 1nmol/well siphonaxanthin for 1, 3, 6 and 24 h. The concentreation of siphonaxanthin in the cells,

medium and the total culture (cells + medium) was determined by HPLC analysis as described in experimental methods. Values are means ± SEMs, n = 3. Data were analyzed by 1-factor ANOVA with repeated measures. Labeled means without a common letter are significantly different within cells, medium and the total culture, respectively, $P< 0.05$.

Analysis of siphonaxanthin metabolites in Caco-2 cells

The representative HPLC chromatogram of an extract of Caco-2 cells after 24 h of incubation with micelles containing siphonaxanthin was shown in the **Fig. 2-2B.** The most predominant peak at about 30 min (peak 3) was completely fitted with the peak corresponding to the standard of siphonaxanthin (**Fig. 2-2A**). The peak 3 was identified as siphonaxanthin based on its UV-vis spectrum (Fig. 2-3A) and characteristic ions at charge ratio (*m/z*) 583 $[M+H-H_2O]^+$, 565 $[M+H-2H_2O]^+$ and 547 $[M+H-3H_2O]^+$ by APCI (Fig. 2-3B) and 623 $[M+Na]^+$ by ESI. The peak 4 appeared in the HPLC chromatogram of the cell extract (**Fig. 2-2B**). The APCI-MS spectrum of peak 4 showed the same ion peaks with siphonaxanthin (**Fig. 2-3A**); however, its UV-vis spectrum presented a strong *cis* peak at 331 nm (**Fig. 2-3B**). The peak 4 was identified as *cis*-siphonaxanthin. Excepted for peak 1 and 4, no additional peaks were detected during incubation for 1-6 h (data not shown). However, after incubation for 24 h with siphonaxanthin, the peaks 1, 2, and 5 appeared in the HPLC chromatogram of the cell extract (**Fig. 2-2B**). The UV-vis spectrum of peak 1 with maximum absorbance at 452 nm was almost consistent with that of siphonaxanthin. The APCI-MS spectrum showed the ion peaks at m/z 599 $[M+H]^+$, 581 $[M+H-H_2O]^+$, 563 $[M+H-2H_2O]^+$, and no further product ion based on loss of water in the MS/MS spectrum of the m/z 563 fragment as a precursor ion, indicating the presence of two hydroxyl groups and the presumable generation of a keto group from dehydrogenation of a hydroxyl group in a C40 carotene backbone. The ESI-MS also showed the ion peak at m/z 621$[M+Na]^+$, indicating its possible molecular mass is 598. The peak 2 at

25 min was detected in the cells extract (**Fig. 2-2B**). The maximum absorbance of peak 2 shifted to long-wavelength compared with that of the siphonaxanthin (**Fig. 2-3A**). The mass spectrum of peak 2 showed two fragment ions at m/z 581 $[M+H-H_2O]^+$ and 563 $[M+H-2H_2O]^+$; however, the ion peak at m/z 599 $[M+H]^+$ was not observed, indicating that the position of keto group generated by dehydrogenation of hydroxyl group is different from that of peak 1. These two compounds corresponding to peak 1 and 2 were assumed to be the dehydrogenation metabolites of siphonaxanthin, didehydro-siphonaxanthin.

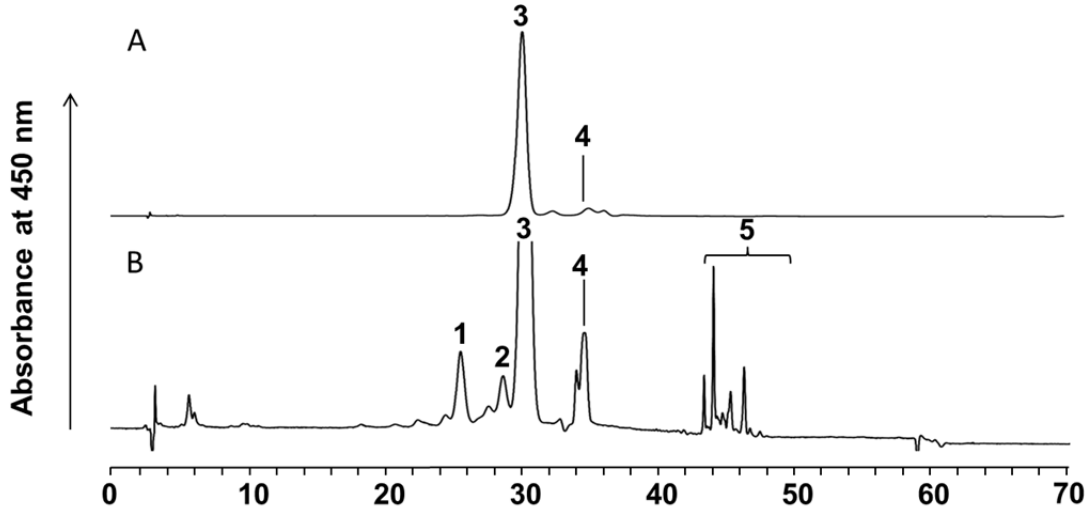

FIGURE 2-2 Representative HPLC chromatograms of the micelles containing siphonaxanthin (A) and the extract from Caco-2 cells after treatment of siphonaxanthin-containg micelles for 24 h (B). The HPLC analysis was performed as described in experimental methods. Peaks: 1, 2 and 5, unknown metabolites; 3, siphonaxanthin; 4, cis isomer of siphonaxanthin. The detection wavelength was 450 nm.

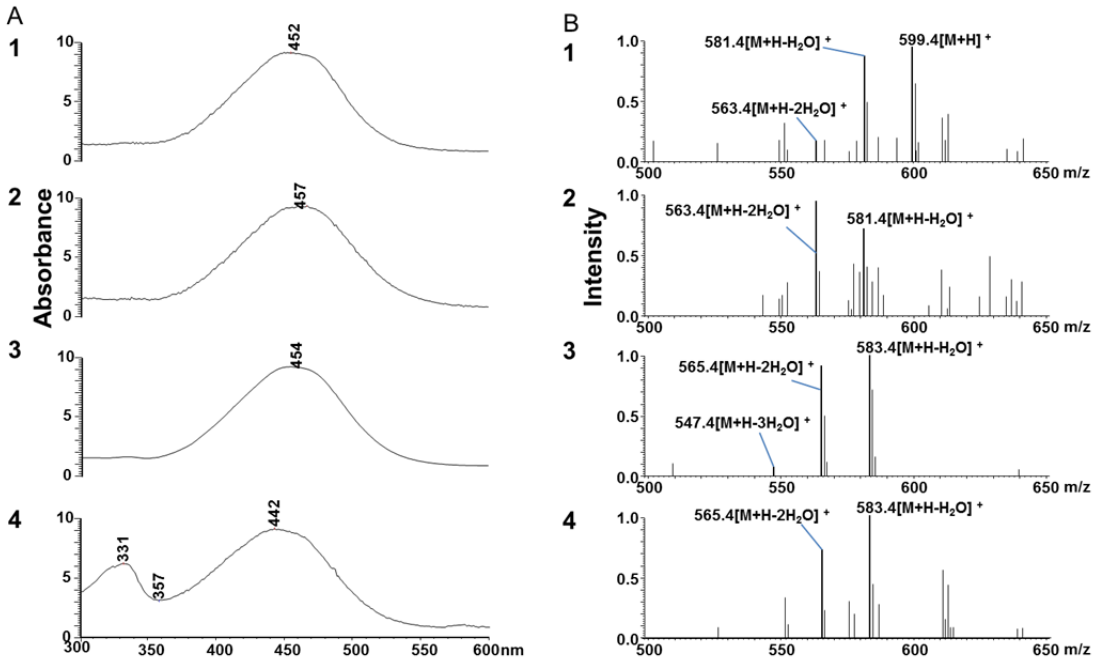

Figure 2-3 UV-vis spectra (A) and APCI-MS spectra (B) of peaks in **Fig. 2-2B**. The LC-MS with APCI analysis was performed as described in experimental methods.

Body weight, feed and tissues weight

The body weight of mice fed siphonaxanthin was not altered compared with the mice fed the control diet (**Fig. 2-4A**). During the 16-day test period, the food intake was not changed between the control and siphonaxanthin group (**Fig. 2-4B**). Siphonaxanthin supplementation significantly decreased the weight of spleen compared to the control diet (**Fig. 2-4C**). The weight of the other tissues was not significantly different between the siphonaxanthin and control groups (**Fig. 2-4C**).

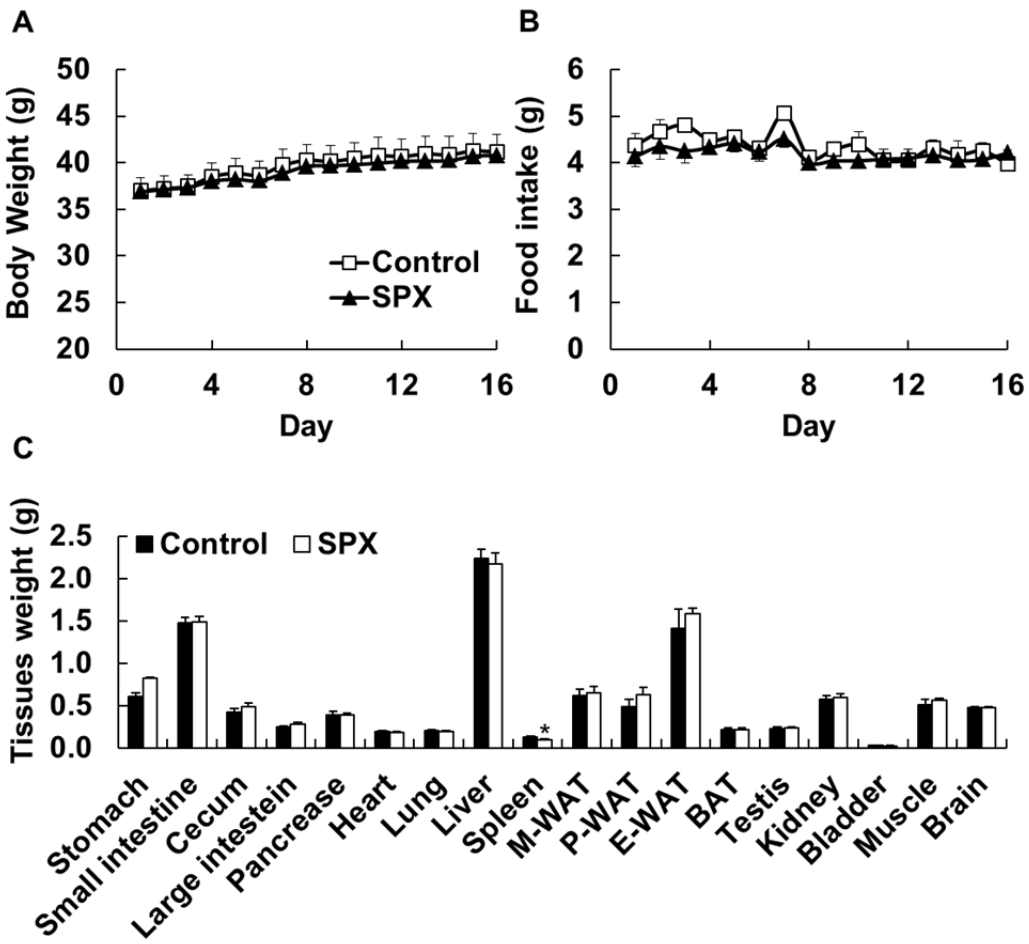

FIGURE 2-4 body weight (A), food intake (B) and tissues weights (C). in ICR mice. ICR mice were fed control or siphonaxanthin supplementation diet for 16 days. Body weight and food intake were measured every day. After 16-day of feeding, the mice were killed and the weight of tissues was measured. Values are means ± SEMs, n = 4. The difference between control and siphonaxanthin group was analyzed by using Student's *t* test. *Different from the control group, $P < 0.05$. BAT, brown adipose tissue; WAT, white adipose tissue.

Analysis of siphonaxanthin metabolites in mice

The representative HPLC chromatograms of the extract from each tissue of mouse fed diet containing siphonaxanthin for 16 days were shown in the **Fig. 2-5.** The peaks 1, 2, 3, 4 and 5 appeared in HPLC chromatogram of the extract from most tissues of mice. The peak 4 at

about 30 min was identified as siphonaxanthin based on its UV-vis and MS spectra (**Fig. 2-6)**. Siphonaxanthin underwent a wide distribution from blood into tissues, except for the bladder. The UV-vis and APCI-MS spectra of peak 2 and peak 3 were absolutely same with the peaks eluted at 25 and 28 min found in the cell extract treated with siphonaxanthin, respectively. Thus, the two compounds were identified as the same metabolites with that found in the Caco-2 cells, didehydro-siphonaxanthins. The maximum absorbance at 459 nm of peak 1 shifted to long-wavelength compared with that of the siphonaxanthin (**Fig. 2-6A)**. The APCI-MS spectrum showed the ion peaks at m/z 597$[M+H]^+$ and 579 $[M+H-H_2O]^+$, and no further product ion based on loss of water in the MS/MS spectrum of the m/z 579 fragment as a precursor ion (**Fig. 2-6B)**, indicating the presence of one hydroxyl group and the presumable generation of two keto groups from dehydrogenation of two hydroxyl groups in a C40 carotene backbone. The ESI-MS also showed the ion peak at m/z 619$[M+Na]^+$, indicating its possible molecular mass is 596. This compound corresponding to peak 1 was assumed to be the dehydrogenation metabolites of siphonaxanthin, tetradehydro-siphonaxanthin. The UV-vis spectrum of peak 5 with maximum absorbance at 455 nm was almost consistent with the siphonaxanthin (**Fig. 2-6A)**. The APCI-MS spectrum showed the ion peaks at m/z 581 $[M+H-H_2O-x]^+$, 563 $[M+H-2H_2O-x]^+$ (**Fig. 2-6B)**; however its retention time was more back at 41 min, the structure of compound was not supposed under the present results.

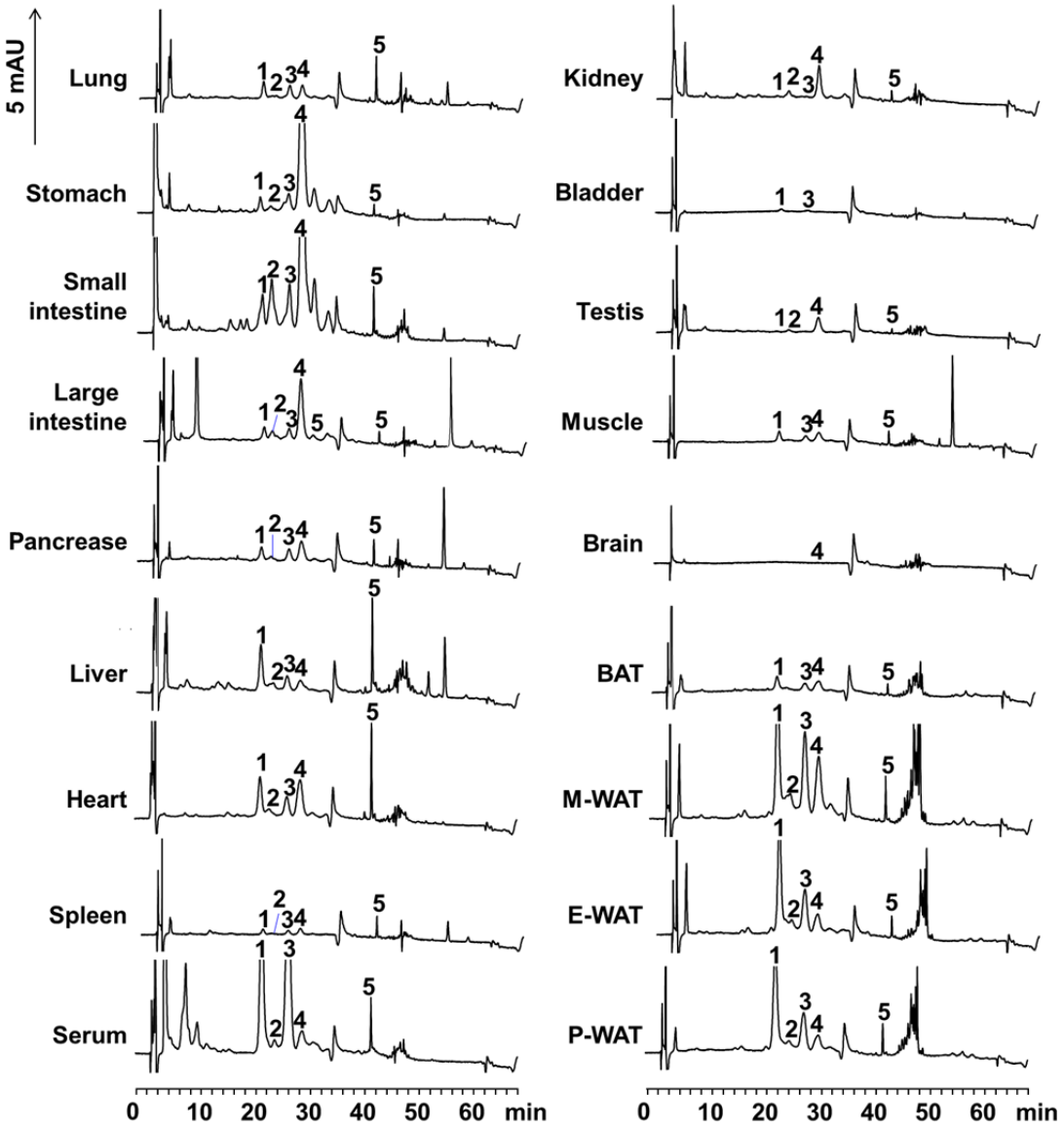

FIGURE 2-5 Representative HPLC chromatograms of the extract from each tissue of mouse fed diet containing siphonaxanthin for 16 days. The HPLC analysis was performed as described in experimental methods. The detection wavelength was 450 nm. Peaks with the same number in different chromatograms had similar UV-vis and MS spectra, shown in the **Fig. 2-6A&B**.

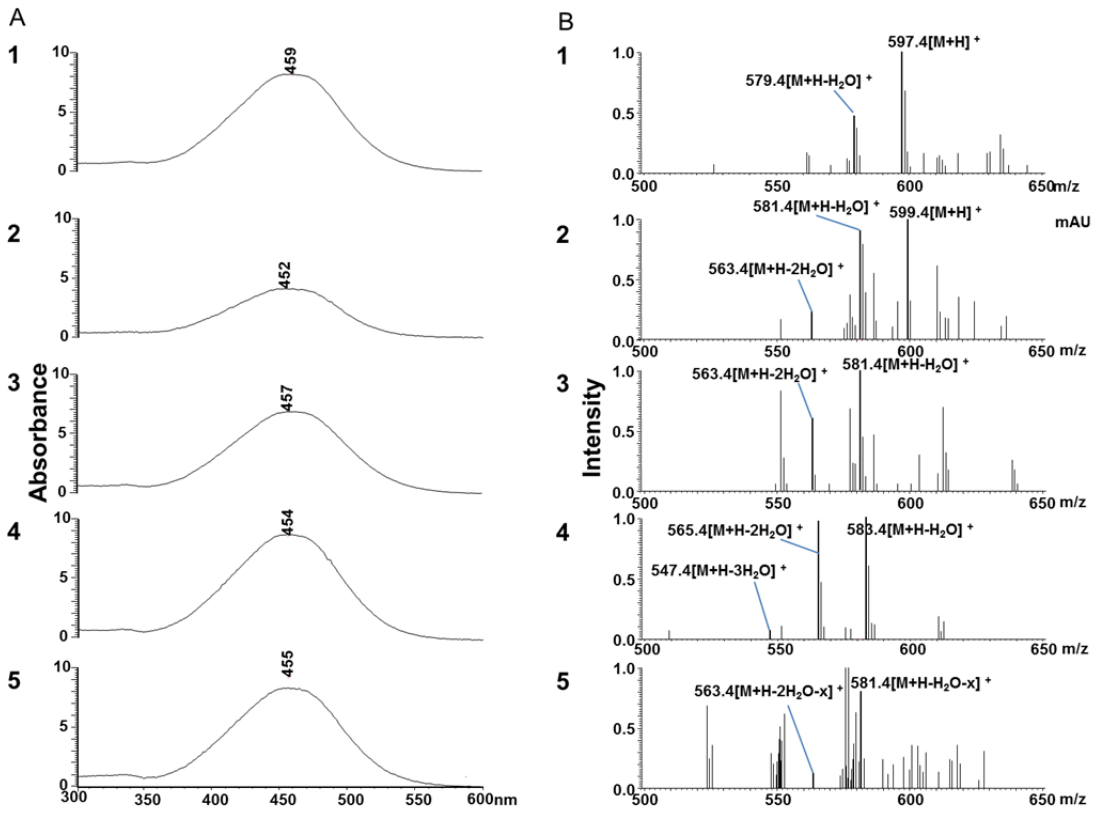

FIGURE 2-6 UV-vis spectra (A) and APCI-MS spectra (B) of peaks detected in **Fig. 2-5**. The LC-MS (APCI) analysis was performed as described in experimental methods.

Tissue distribution and accumulation of siphonaxanthin and its metabolites in mice

At the end of the dietary supplementation with siphonaxanthin, a higher concentration of intact siphonaxanthin was detected in small intestine, stomach and colon than in plasma and the other tissues (**Table 2-1**). It is notable that the concentration of siphonaxanthin in mesenteric WAT was higher than in the epididymal and perirenal WAT (**Table 2-1**). In addition, siphonaxanthin was observed to accumulate in mice brain, although the concentration was very low (**Table 2-1**).

Siphonaxanthin metabolites were quantified by using the standard curve of siphonaxanthin (**Table 2-1**). After the dietary supplementation with siphonaxanthin, the concentration of

metabolite corresponding to the peak 2 was relatively higher in small intestine than mesenteric WAT. The metabolite corresponding to the peak 3 was preferentially accumulated in small intestine > serum > WATs > liver. The metabolite corresponding to the peak 1 mainly accumulated in mesenteric WAT > small intestine > serum > liver > perirenal and epididymal WATs. Among the WATs and liver, the proportion of these metabolic compounds were more than 50% of total, while the proportion was less than 30% in the small intestine, stomach and colon (**Table 2-1**).

TABLE 2-1 Concentration of siphonaxanthin and its metabolites in plasma and tissues of mice at the end of the 16-day dietary supplementation with siphonaxanthin[1].

Tissue	Peak1	Peak2	Peak 3	Siphonaxanthin	Total
Stomach, pmol/g (%)	26.6 ± 13.5 (1.2)	19.0 ± 3.3 (0.9)	86.1 ± 11.0 (3.9)	2054 ± 636 (94.0)	2186 ± 612
Small intestine, pmol/g (%)	172 ± 114 (4.0)	287 ± 132 (6.7)	423 ± 273 (9.8)	3428 ± 1389 (79.5)	4310 ± 1837
Pancreas, pmol/g (%)	24.7 ± 14.3 (24.3)	6.4 ± 3.8 (6.3)	24.4 ± 14.1 (24.0)	46.1 ± 12.5 (45.4)	102 ± 44.2
Spleen, pmol/g (%)	10.5 ± 5.2 (23.2)	2.9 ± 1.0 (6.4)	11.1 ± 4.9 (24.7)	20.6 ± 3.4 (45.7)	45.1 ± 12.5
Colon, pmol/g (%)	12.3 ± 7.5 (5.1)	8.7 ± 0.4 (3.6)	20.9 ± 11.4 (8.7)	198 ± 24.5 (82.5)	239 ± 11.3
Lung, pmol/g (%)	18.3 ± 10.8 (30.9)	0.6 ± 0.4 (1.0)	17.3 ± 10.0 (29.3)	22.9 ± 8.2 (38.8)	59.0 ± 29.3
Heart, pmol/g (%)	35.0 ± 20.2 (27.2)	4.6 ± 2.6 (3.5)	21.9 ± 12.7 (17.0)	67.1 ± 25.2 (52.2)	129 ± 60.6
Liver, pmol/g (%)	110 ± 63.4 (55.3)	11.3 ± 4.6 (5.7)	40.3 ± 21.2 (20.3)	37.1 ± 14.4 (18.7)	198 ± 102
Bladder, pmol/g (%)	14.6 ± 8.5 (58.5)	N.D.	10.4 ± 6.1 (41.5)	N.D.	25.0 ± 14.6
Muscle, pmol/g (%)	9.9 ± 5.7 (36.5)	0.7 ± 0.7 (2.6)	2.2 ± 2.2 (8.3)	14.2 ± 7.5 (52.6)	27.1 ± 15.1
Serum, pmol/mL (%)	162 ± 93.4 (48.8)	3.5 ± 2.0 (1.0)	147.4 ± 78.6 (44.6)	18.3 ± 4.0 (5.5)	331 ± 177
BAT, pmol/g (%)	25.3 ± 15.4 (34.6)	0.6 ± 0.6 (0.8)	16.7 ± 9.5 (22.9)	30.5 ± 11.4 (41.7)	73.1 ± 36.0
Mesenteric WAT, pmol/g (%)	188 ± 106 (41.8)	43.6 ± 21.8 (9.7)	108.1 ± 58.7 (24.0)	110 ± 50.8 (24.5)	449 ± 236
Perirenal WAT, pmol/g (%)	95.5 ± 62.2 (57.4)	4.3 ± 2.5 (2.6)	44.4 ± 29.4 (26.7)	22.1 ± 12.0 (13.3)	166 ± 105
Epididymal WAT, pmol/g (%)	112 ± 69.0 (58.9)	N.D.	50.6 ± 30.3 (26.5)	27.8 ± 14.3 (14.6)	190 ± 113
Kidney, pmol/g (%)	0.5 ± 0.5 (1.0)	6.6 ± 2.9 (14.6)	0.1 ± 0.1 (0.3)	38.2 ± 15.7 (84.1)	45.4 ± 18.9
Testis, pmol/g (%)	1.2 ± 0.8 (4.1)	3.0 ± 1.8 (10.2)	0.4 ± 0.4 (1.3)	25.0 ± 10.0 (84.3)	29.6 ± 12.6
Brain, pmol/g (%)	N.D.	N.D.	N.D.	0.4 ± 0.3 (100)	0.4 ± 0.3

[1] The quantification of siphonaxanthin and metabolites was based on the peaks area in the HPLC chromatogram. The values in parenthesis for siphonaxanthin (peak 4) and metabolites (peak 1-3) is also expressed as % of the total carotenoids. Values are means ± SEMs, n = 4. BAT, brown adipose tissue; WAT, white adipose tissue; N.D., not detected.

DISCUSSION

Studies on the bioavailability and biotransformation of dietary carotenoid are requisite in order to increase an understanding of their potential health benefits. In this chapter, the metabolism, distribution and accumulation of dietary siphonaxanthin were investigated. It is found that metabolites of siphonaxanthin were generated in differentiated Caco-2 cells. Several siphonaxanthin metabolites were detected in the plasma and tissues of ICR mice after 16-day siphonaxanthin supplementation.

The finding in this chapter indicated that siphonaxanthin was oxidized into two kinds of didehydro-siphonaxanthins in the differentiated Caco-2 cells. It is suggested that siphonaxanthin is derived from lutein via oxidation pathway among green algae (6). Lutein has been reported that its metabolites, keto-carotenoids, are detected in plasma and tissues of mice and human (80). Due to similar chemical structures between lutein and siphonaxanthin, it was assumed that the possible structures of the two siphonaxanthin metabolites found in Caco-2 cells were considered as dehydrogenization products of siphonaxanthin, didihydro-siphonaxanthins, in which a hydroxyl group might be oxidized into a keto group. Siphonaxanthin have three hydroxyl groups at the position of 3, 19 and 3', all of which may be oxidized into keto group. However, the oxidation of lutein at 3 and 3' position (80), the oxidation of capsanthin at 3' position to capsanthone (81), and the dehydrogenation of fucoxanthinol at 3 position to amarouciaxanthin in mice liver (22) after ingestion of those carotenoids *in vivo* were reported. These above reports indicate the position at β or ε-end ring might be liable to be oxidized. Thus, the two dehydrogenated metabolites of siphonaxanthin were presumed to be 3'-oxo-siphonaxanthin or 3-oxo-siphonaxanthin (**Fig. 2-7**)； However, in the present study, the difference of the two metabolites still uncertain.

Since the same oxidative metabolites were found in both Caco-2 cells and small intestine, siphonaxanthin might be converted to 3-oxo-siphonaxanthin or 3'-oxo-siphonaxanthin by dehydrogenase present in the small intestine. In addition, the two metabolites were found in plasma and the other tissues. Also of note, the compound for peak 3 (**Fig. 2-5)** was more abundant than peak 2 (**Fig. 2-5)** in the most tissues, especially in the serum and WATs (**Table 2-1**), which indicated that the structure of the compound for peak 3might be more stable *in vivo*. It have been reported that the metabolites of lutein 3'-hydroxyl-β,ε-caroten-3-one which was detected to be largely accumulated in mice tissues was more stable than 3-hydroxyl-β,ε-caroten-3'-one which was just detected in the human serum (80). Thus, the, peak3 (**Fig. 2-5)** was presumed to be 3-oxo-siphonaxanthin.

Another finding was that the metabolite eluted at 22 min was the most abundant metabolite and accounted for 40-60% of the metabolites in mice serum, liver and WATs. Based on the MS spectra, the metabolite was also considered as dehydrogenization product of siphonaxanthin, tetradihydro-siphonaxanthin. It is speculated that two hydroxyl groups were transformed into two keto groups in the structure of the metabolite. Similar to the oxidative metabolite of lutein and fucoxanthinol described above, 3 and 3' position at β- or ε-end ring is possible oxidation positions in the carotenoid structure. Others authors have reported that oxidation of 4,4'-dimethoxy-β-carotene were oxidized into 4,4'-diketo-β-carotene in human subjects (82). Thus, this metabolite eluted at 22 min is most likely identified as 3, 3'-dioxo-siphonaxanthin (**Fig. 2-7**).

Furthermore, the metabolites eluted at about 42 min were assumed as the ester of siphonaxanthin or other siphonaxanthin metabolites. Peridinin is hydrolyzed to its fatty acid esters in the differentiated Caco-2 cells (83). There is no available information about the fatty acid esters of carotenoids in the mice. At present, due to the existence of triacylglycerol in the

extract from cells and mice, the identification for the metabolite is difficult. The intriguing metabolite needs identification in the future study. The metabolic pathway of lutein and zeaxanthin has been suggested in many reports (84-86). Due to similarity between the structure of siphonaxanthin and lutein, based on the results in the study and aforementioned reports the following metabolic pathway for siphonaxanthin was assumed (**Fig. 2-7**): siphonaxanthin to 3,3'-Dioxo-siphonaxanthin (19-Hydroxy-7,8-dihydro-ε,ε-caroten-3,8,3'-trione) via 3-oxo-siphonaxanthin (19,3'-Dihydroxy-7,8-dihydro-β,ε-caroten-3,8-dione) or 3'-oxo-siphonaxanthin (3,19-Dihydroxy-7,8-dihydro-β,ε-caroten-8,3'-dione).

One acknowledged aspect of carotenoid action *in vivo* is the inconsistency of distribution of carotenoids among tissues (73). The major site of distribution is not identical for different carotenoid, and the distribution is different even for the same carotenoid due to the experimental condition, such as supplementation period. Fucoxanthin and its metabolites mainly accumulated in the adipose tissues and its metabolites amarouciaxanthin A preferentially accumulated in the adipose tissues (87). Lutein and β-carotene have been reported mainly accumulated in the liver instead of adipose tissues (73, 80). In the present study, siphonaxanthin was not completely metabolized in the gastrointestinal tract and absorbed into the body as its metabolite, whereas in contrast, siphonaxanthin were detected in the plasma and most tissues except bladder after 16-day feeding period. Canthaxanthin, lycopene, and carotene have been reported to accumulate in the colon and small intestine by a small quantity (73). Surprisingly, siphonaxanthin was mainly concentrated in the small intestine, stomach and large intestine, which was considered that siphonaxanthin might stick on the intestinal mucosa, rather than accumulated in the intestine. Another factor might be that the mice were not food-deprived before sacrificed in this study. Notably, siphonaxanthin were more easily accumulated in mesenteric adipose tissue instead of epididymal WAT, perirenal

WAT and BAT, which might be attributed to that the mesenteric WAT is more close to the digestion gastrointestinal tract. The results are consistent with the finding in the chapter 1, that siphonaxanthin mainly accumulated in the KK-Ay mice administrated with siphonaxanthin for 6 weeks.

The distribution profile of each metabolite monomer differed among tissues. The metabolite of peak3 (**Fig. 2-5**) and 3,3'-dioxo-siphonaxanthin were more abundant than siphonaxanthin in liver, serum and WATs, whereas the others tissues presents the opposite condition. The metabolite of peak2 (**Fig. 2-5**) mainly accumulated in the small intestine, whereas the other tissues had small amounts of this metabolite. The different distribution of siphonaxanthin metabolites in tissues might be associated with specific enzyme present in different tissues and the metabolic and transport rate of each metabolite.

Althrough further efforts are needed to clarify the enzymes and metabolic mechanisms involved in the oxidative pathway for siphonaxanthin, here, the fact that keto-carotenoids is the main metabolites of siphonaxanthin which could accumulate in the body are found for the first time. The keto-carotenoids possibly derived from siphonaxanthin have a unique structure containing α,β-unsaturated carbonyl moiety, which has high potential reacting with nucleophilic molecules in the tissues (88). Therefore, in order to understand the role of siphonaxanthin on human health, bioactivity of siphonaxanthin metabolites is worth evaluating.

In summary, the keto-carotenoids 3-oxo-siphonaxanthin, 3'-oxo-siphonaxanthin, and 3,3'-dioxo-siphonaxanthin were identified as major metabolites of dietary siphonaxanthin in ICR mice. The study also speculated the possible metabolic pathway for siphonaxanthin *in vivo* and showed the non-uniform tissue accumulation and distribution profile of siphonaxanthin and its metabolites. Although further studies are needed for siphonaxanthin metabolic

mechnisms, the study has provided useful information for the studies on effects of siphonaxanthin on human health.

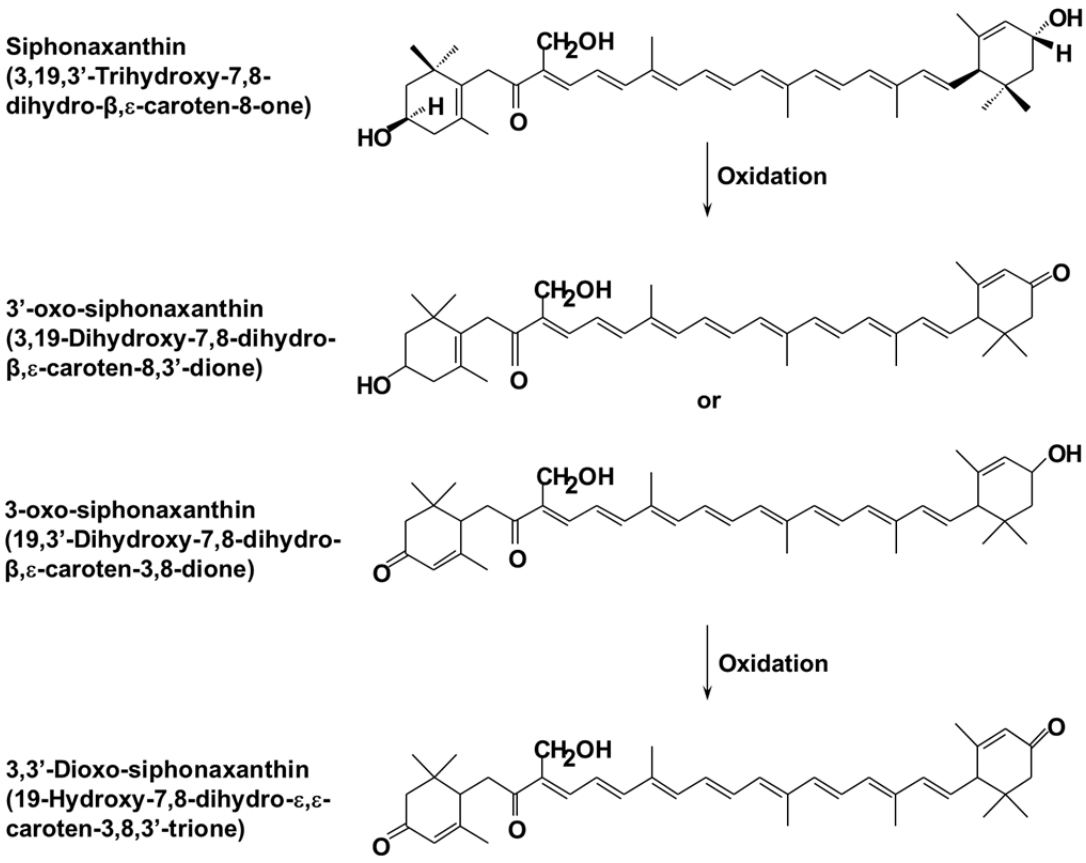

FIGURE 2-7 Name and molecular formula of proposed siphonaxanthin metabolites, and proposed pathway for siphonaxanthin metabolism in mice.

INTRODUCTION

Siphonaxanthin is a natural keto-carotenoid found in several edible green algae. In the chapter1 siphonaxanthin was found to inhibit adipogenesis in 3T3-L1 preadipocytes and lipid accumulation in white adipose tissue of KK-Ay mice. The results in the chapter1 indicate that siphonaxanthin potently suppressed the differentiation of 3T3-L1 cells via the down-regulation of key adipogenesis genes, including *Cebpa*, *Pparg*, *Fabp4* and *Scd1*. Moreover, oral administration of siphonaxanthin to KK-Ay mice significantly reduced the weight of the mesenteric white adipose tissue (WAT) via reducing lipogenesis and enhancing fatty acid oxidation in the adipose tissue. The inhibitory effect of siphonaxanthin on the adiposity of mesenteric WAT was attributed to its selective high accumulation in the WAT.

Siphonaxanthin specifically presents in some green algae which can live in the deeper water, such as *Codium fragile*, *Caulerpa lentillifera*, *Umbraulva japonica* and *Codium cylindricum*. The content of siphonaxanthin in the above-mentioned algae is almost 20-230 μg/g. The purification of siphonaxanthin from the algae is technically complicated, and as supplement, the acquisition for a large amount of siphonaxanthin is currently impossible. Thus, direct application of siphonaxanthin-rich green algae might be promising strategy. However, the information about the benefits of dietary green algae to obesity is still poorly understood.

Brown algal carotenoid, fucoxanthin, has been revealed to have a remarkable anti-obesity property in mice, rats and human subjects (12, 89). The supplementation of fucoxanthin-rich edible brown algae, such as tororokombu (*Sargassum polycystum*) has been reported to inhibit the development of obesity (90, 91). The anti-obesity effect of fucoxanthin has been recognized to contribute to the inhibitory effect of above brown algae on obesity (90, 91). In

addition, both fucoxanthin-rich seaweed extract and purified fucoxanthin are equally effective on reducing adipose tissue weight and regulating lipid metabolism (40, 41).

The content of siphonaxanthin in *Codium cylindricum* is relatively higher than other species of edible green algae. Thus, in this chapter, the siphonaxanthin-rich green alga, *Codium cylindricum*, was used to evaluate its anti-obesity effect. The effect of dietary *Codium cylindricum* powder on obesity was investigated by using high-fat diet-induced obese C57BL/6J mice model. The underlying molecular mechanisms involved in the lipid metabolism were further elucidated. In addition, to understand the possible role of siphonaxanthin in dietary green algae, the accumulation of siphonaxnathin in the WAT was determined. The findings in this chapter provide the possibility for new application of siphonaxanthin-rich green algae as functional foodstuff.

MATERIALS AND METHODS

Preparation of green algal powder

Edible green alga (*Codium cylindricum*) used in this study was kindly donated from the Mie Prefecture Fisheries Research Institute, Japan. After thoroughly washing with water to remove debris, epiphytes and salt, the alga was frozen-dried and pulverized using a grinder into fine powder. The sample was stored at -20°C until required. The nutrient composition of algal powder was analyzed (**Table 3-1**).

TABLE 3-1: Nutrient composition of dried powder of *Codium cylindricum*.

Nutrient	Fresh	Dried
Moisture content (%)	96	2.5
Protein (%)	0.8	19.5
Fat (%)	0.2	4.9
Ash (%)	0.3	7.3
Carbohydrate (%)	2.7	65.8
Dietary fiber (%)	2.9	70.7
Energy (kcal)	8	192.5

Animals and diets

All experimental animal protocols were approved by the Animal Experimentation Committee of Kyoto University for the care and use of experimental animals. Male C57BL/6J mice (4 weeks of age) were purchased from Charles River Laboratories Japan, Inc. (Tokyo, Japan). All mice were housed individually in plastic cages and maintained on an alternating 12-h light/dark cycle at a temperature of 23 ± 1°C. After an acclimatization period of 1 week, the

mice were randomly divided into 4 experimental groups (n = 6 per group). The low-fat fed-group (LF) was fed with the purified diet (AIN-93G diet) containing 7 wt% fat (45). The high-fat fed-group (HF) was fed a modified AIN-93G diet containing 35 wt% fat (**Table 3-2**), and the other two groups were fed the HF diet supplemented with 1 or 5 wt% frozen-dried green alga powder (1GA or 5GA). The body weights and food consumption of mice were recorded every day throughout the study. After 78 days of dietary treatments, mice were feed-deprived for 16 h and killed under isoflurane anesthesia. Blood was collected, and organs including white and brown adipose tissues, liver, and muscle were rapidly removed, weighed, and stored in RNA laterTM solution (Ambion Inc., USA).

TABLE 3-2: Composition of normal diet and high fat diet.

	Diet	
Ingredient	AIN-93G	HFD-60
	U/kg diet	
Casein (g)	200	256
L-cystine (g)	3	3.6
Maltodextrin (g)	0	60
Cornstarch (g)	397.486	0
Dextrinized cornstarch (g)	132	159.992
Sucrose (g)	100	55
Soybean oil (g)	70	20
Lard (g)	0	330
Cellulose (g)	50	66.1
Mineral mix (g)	35	35
Calcium carbonate (g)	0	1.8
Vitamin mix (g)	10	10
Choline bitartrate (g)	2.5	2.5
BHT (g)	0.014	0.008
Total energy (kcal)	3999.9	5328.4
Fat (kcal%)	15.8	59.1

Measurement of serum biochemical parameters

The serum was prepared by centrifuging at 400 × g for 15 min at 4°C, and stored at -80 °C until analysis. Serum levels of triacylglycerol (TG), free cholesterol, total cholesterol (TC), HDL-cholesterol (HDL-C), nonesterified fatty acid (NEFA), aspartate aminotransferase (AST), alanine aminotransferase (ALT), and glucose were determined using commercially available kits (TG E, F-Cho E, T-Cho E, HDL-C E, NEFA C, GOT·GPT C II, Glu C II; Wako Pure Chemical Industries, Ltd., Osaka, Japan).

Measurement of TG and TC levels in the liver and feces

Aliquot liver samples of each group were homogenized in 9-fold volume of 0.9% NaCl saline with a teflon-glass homogenizer. Hepatic lipids were extracted from each homogenate with chloroform/methanol (2:1, v/v). Feces were collected on a per-cage basis for 24 h after 35 days of feeding. Feces were ground under liquid nitrogen with a porcelain mortar and pestle until a fine powder was obtained. Fecal total lipids were then extracted with H_2O/chloroform/methanol (0.9:2:1, v/v/v). The lipid samples were dissolved in methanol containing 50% Triton X-100 and then assay for TG, TC and NEFA levels using a commercial enzymatic kit as mentioned above, respectively.

RNA extraction and quantitative real-time RT-PCR

Total RNA was extracted from the frozen tissues by using Sepasol®-RNA I Super G (Nacalai Tesque, Japan) as described in the manufacturer's instructions, and was treated with DNase (Wako Pure Chemical Industries, Ltd., Osaka, Japan). Then, 2 μg of total RNA from each sample was reverse-transcribed to cDNA by using SuperScript RNase II reverse transcriptase kit (Invitrogen Corp., USA) with random hexamers. For RT-PCR, cDNA was diluted and

mixed with iQ SYBR green supermix (Bio-Rad Laboratories, Hercules, CA, USA) containing 1 μmol/L PCR primer. Primers used for the quantification of each gene are listed in **Table 3-3**. Quantitative Real-time PCR was performed using a DNA Engine Option system (Bio-Rad Laboratories, Hercules, CA, USA). The PCR protocol included the following thermal cycling conditions: one cycle at 95°C for 15 min, followed by 43 cycles at 95°C for 15 s and 60°C for 30 s. The mRNA expression level of each gene was normalized to *Gapdh* expression.

TABLE 3-3: GenBank accession numbers and primer sequences used in RT-PCR experiments.

Gene	sense(5'-3')	Anti-sense(5'-3')	Gene number
Acox1	ACCTTCACTTGGGCATGTTC	TTCCAAGCCTCGAAGATGAG	NM_015729.3
Adipoq	GTTCTACTGCAACATTCCGG	TACACCTGGAGCCAGACTTG	NM_009605.4
CPT1a	CTCCGCCTGAGCCATGAAG	CACCAGTGATGATGCCATTCT	NM_013495.2
Fas	CCTGGAACGAGAACACGATCT	AGACGTGTCACTCCTGGACTTG	NM_007988.3
Gapdh	CGTCCCGTAGACAAAATGGT	TGCCGTGAGTGGAGTCATAC	NM_008084.2
G6pd	GGTACCTACAAGTGGGTGAA	AGATGGTGAAAAGGGAAGAT	NM_008062.2
Pgc1a	GAAGTGGTGTAGCGACCAATC	AATGAGGGCAATCCGTCTTCA	NM_008904.2
Pgc1b	TCCTGTAAAAGCCCGGAGTAT	GCTCTGGTAGGGGCAGTGA	NM_133249.2
Ppara	GTACGGTGTGTATGAAGCCATC	GCCGTACGCGATCAGCAT	NM_011144.6
Pparg	GCCCTTTGGTGACTTTATGG	GGCGGTCTCCACTGAGAATA	NM_011146.3
Scd1	ACAGTCCAGGGCCAACAGT	GGCACCTTACACAGCCAGTT	NM_009127.4
Srebp1c	GGAGCCATGGATTGCACATT	GCTTCCAGAGAGGAGCCCAG	NM_011480

Measurement of siphonaxanthin content in dried green algal powder and biological samples

Carotenoids were extracted from algal powder, feces, WATs and liver. Briefly, the aliquots of tissue sample (0.2g) were homogenized in a 9-fold volume of 0.9% NaCl saline with a homogenizer dispenser (T10 basic ULTRA-TURRAX, IKA). To extract carotenoid, the resultant tissue homogenates (0.9 mL) were mixed with 3 mL of dichloromethane/methanol

(2:1, v/v). Freeze-dried algal powder (0.03g) and mice fecal powder (0.1 g) described as above were mixed with 3.9 mL of water/dichloromethane/methanol (0.9:2:1, v/v/v), respectively. The samples were extracted three times, and the dichloromethane layer was collected after centrifugation at 1690 g at 4°C for 15 min. After evaporation under nitrogen, the residue was resuspended in 100 μL of dichloromethane/methanol (1:1, v/v) for HPLC analysis.

HPLC analysis

HPLC analysis was carried out with a Prominence LC system (Shimadzu, Kyoto, Japan), connected to a photodiode array detector (SPD-M20A, Shimadzu) followed by an ion trap-time of flight mass spectrometer (LCMS-IT-TOF, Shimadzu) equipped with an atmospheric pressure chemical ionization (APCI) source. Carotenoids were separated on a TSK gel ODS-80Ts QA column (2.0 × 250 mm, 5μm, Tosoh, Japan). The mobile phase was methanol/water (72:15, v/v) containing 0.1% ammonium acetate at a flow rate of 0.2 mL/min. The peak identities for siphonaxanthin were confirmed from their characteristic UV-VIS spectra recorded and positive ions recorded. Siphonaxanthin was quantified from their peak area by use of a standard curve with purified siphonaxanthin.

Statistical analysis

Data analyses were performed by using the statistical program SPSS 16.0 for Windows. Comparisons were made among groups of normally distributed data by using a 1-factor ANOVA followed by Tukey's multiple comparison test. Data with unequal variances were transformed to logarithms. Data are represented as means ± SEMs. Statistical significance was defined as $P < 0.05$.

RESULTS

Effect of dietary green alga on body weight and adiposity

Body weight gain of the four groups of mice was compared after 78 days of feeding (**Fig. 3-1A**). A HF diet resulted in a significant increase in body weight gain of mice compared with a LF diet. The body weight gain of mice fed a HF diet containing 1 or 5% algal powder increased less than that of mice fed a HF diet. The difference became significant from 10 weeks after the dietary treatment in 5GA group. During the experimental period, the food intake was significantly higher in mice fed a LF diet than in mice fed a HF diet, but was not significantly different between the HF and 1GA or 5GA groups (**Fig. 3-1B**). The weights of the mesenteric, perirenal, epididymal and total WAT were significantly increased by the HF diet compared to the LF diet (**Fig. 3-2**). When compared to the HF group, the weight of the epididymal WAT was not changed in algal powder-supplemented mice; however the weight of the perirenal WAT in both 1GA and 5GA groups was significantly decreased, and the weights of mesenteric ($P = 0.06$) and total WAT ($P = 0.09$) tended to be lower in 5GA group (**Fig. 3-2**). On the other hand, the weights of liver and interscapular brown adipose tissue (BAT) did not change among the groups (**Fig. 3-2**).

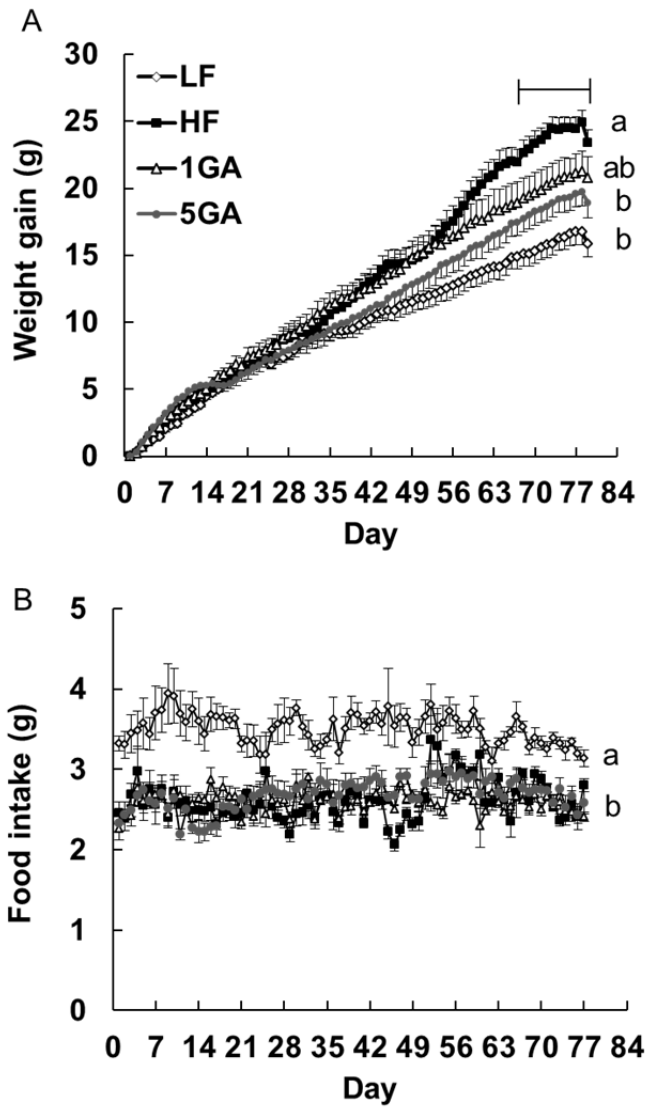

FIGURE 3-1 Time changes of body weight gain and food intake of mice during 78 days of feeding. Values are means ± SEMs, n = 6. Within each graph, labeled means without a common letter are significantly different among groups at $P < 0.05$ as determined by Tukey's test. LF, low fat diet group; HF, high fat diet group; 1GA, 1% green algae powder-supplemented group with a high fat diet; 5GA, 5% green algae powder-supplemented group with a high fat diet.

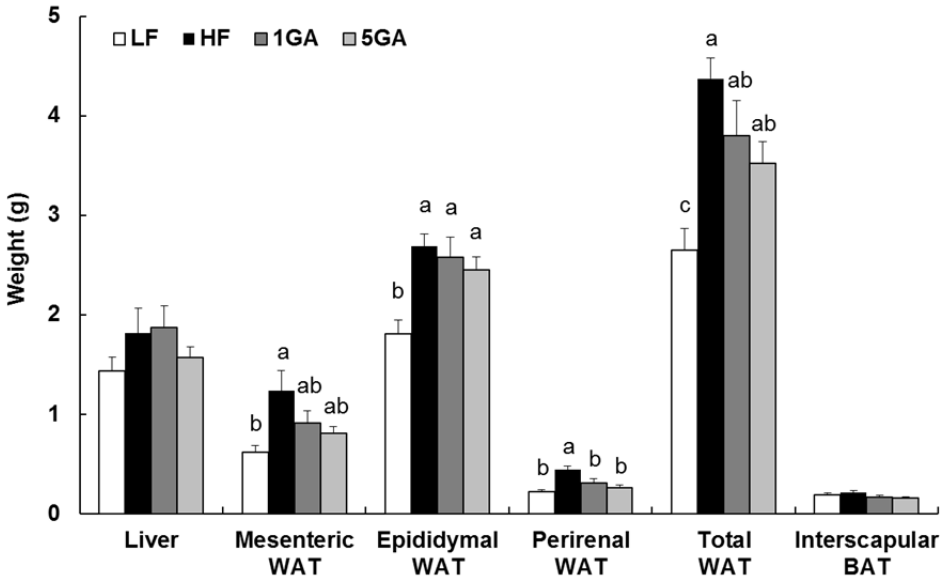

FIGURE 3-2 The weight of liver, WATs and BAT in mice after 78 days of feeding. Values are means ± SEMs, n = 6. Labeled means without a common letter are significantly different among groups at $P < 0.05$ as determined by Tukey's test. WAT, white adipose tissue; BAT, brown adipose tissue. Abbreviations of each group are same as shown in **Fig. 3-1**.

Effects of dietary green alga on parameters in plasma, liver and feces

Table 3-4 shows the major biochemical parameters in plasma, liver and feces. The plasma TG, NEFA, glucose concentrations were not significantly different among the groups. The plasma TC concentrations tended to be lower in the two algal powder supplemented groups than in the HF group ($P = 0.08$ and $P = 0.10$, respectively). The plasma HDL-C concentration was not significantly changed by algal powder supplementation. The HF diet significantly increased plasma AST and ALT activities as compared to the LF diet; in contrast, 5GA group significantly decreased the activities as compared to the HF group.

Hepatic TG concentration was significantly increased in HF group compared to the LF group. Hepatic TC concentration was not significantly different between LF and HF groups;

however, its concentration tended to be lower in 1GA ($P = 0.10$) and 5GA ($P = 0.07$) groups compared to the HF group. Moreover, weight of feces collected for 24h was significantly higher in the 5GA group than in the HF group, and the fecal TG and NEFA concentrations in the 5GA group were significantly elevated compared to the HF group. The fecal TC concentration was not significantly different between the HF group and the algal powder-supplemented groups.

TABLE 3-4: Parameters of plasma, liver and feces in mice after 78 days of feeding.

	LF	HF	1GA	5GA
Plasma TG (mg/dL)	106.1 ± 17.5	72.1 ± 6.9	64.5 ± 7.2	77.5 ± 12.0
Plasma TC (mg/dL)	119.3 ± 4.2^{b}	172.4 ± 6.7^{a}	146.3 ± 10.7^{ab}	147.6 ± 5.4^{ab}
Plasma NEFA (mEq/L)	1.2 ± 0.2	0.8 ± 0.1	0.8 ± 0.1	0.7 ± 0.1
Plasma Glucose (mg/dL)	279.1± 24.4	303.1 ± 10.0	305.1 ± 8.2	262.8 ± 8.2
Plasma HDL-C (mg/dL)	80.3 ± 2.6^{b}	103.4 ± 1.8^{a}	95.9 ± 3.7^{a}	96.1 ± 2.4^{a}
Plasma LDL-C (mg/dL)	17.8 ± 3.9^{b}	54.6 ± 5.7^{a}	37.4 ± 8.1^{ab}	36.0 ± 5.4^{ab}
Plasma ALT (U/L)	9.5±1.2^{b}	26.6±4.1^{a}	17.1± 2.5^{ab}	14.7± 1.8^{b}
Plasma AST (U/L)	27.1 ± 1.8^{b}	49.1 ± 3.9^{a}	35.0 ± 2.6^{b}	31.2 ± 1.9^{b}
Hepatic TG (mg/dL)	77.1 ± 6.2^{b}	95.5 ± 0.7^{a}	61.1± 6.8^{ab}	59.1± 8.8^{ab}
Hepatic TC (mg/dL)	3.5 ± 0.4	3.7 ± 0.3	3.2 ± 0.1	2.6 ± 0.2
Feces (mg/d)	403 ± 30 ^{b}	395 ± 20 ^{b}	442 ± 11^{b}	543 ± 25 ^{a}
Fecal TG (mg/d)	0.3 ± 0.03^{d}	1.0 ± 0.05^{c}	1.2 ± 0.04^{b}	2.6 ± 0.10^{a}
Fecal TC (mg/d)	1.2 ± 0.1^{b}	2.5 ± 0.2^{a}	2.4 ± 0.1^{a}	3.0 ± 0.2^{a}
Fecal NEFA (μEq/d)	1.6 ± 0.1^{c}	4.0 ± 0.3^{b}	4.8 ± 0.1^{b}	5.7 ± 0.2^{a}

Values are means ± SEMs, n = 6. Labeled means without a common letter are significantly different among groups at $P < 0.05$ as determined by Tukey's test. TG, triacylglycerol; TC, total cholesterol; HDL, HDL-cholesterol; LDL, LDL-cholesterol. Abbreviations of each group are same as shown in **Fig. 3-1**.

Effects of dietary green alga on mRNA expression of genes related to lipid metabolism in liver

The mRNA levels of lipid metabolism-related genes in the liver were analyzed by real-time RT-PCR method (**Fig. 3-3**). The mRNA levels of the transcription factor, sterol regulatory element binding protein 1c (*Srebp1c*) and its target gene, fatty acid synthase (*Fas*), which regulate the lipid synthesis in the liver, were not significantly different among the groups. The mRNA level of stearoyl CoA desaturase 1 (*Scd1*), one of the target genes of *Srebp1c*, tended to be lower in 1GA group compared to the HF group (P = 0.06). Furthermore, the mRNA levels of β-oxidation-related genes were also analyzed. The differences in the mRNA expression of peroxisome proliferator-activated receptor alpha (*Ppara*) were not significant among these experimental groups. However, the mRNA levels of carnitine palmitoyltransferase 1 alpha (*Cpt1a*) and acyl-CoA oxidase 1 (*Acox1*) were significantly reduced in 5GA group compared to the HF group.

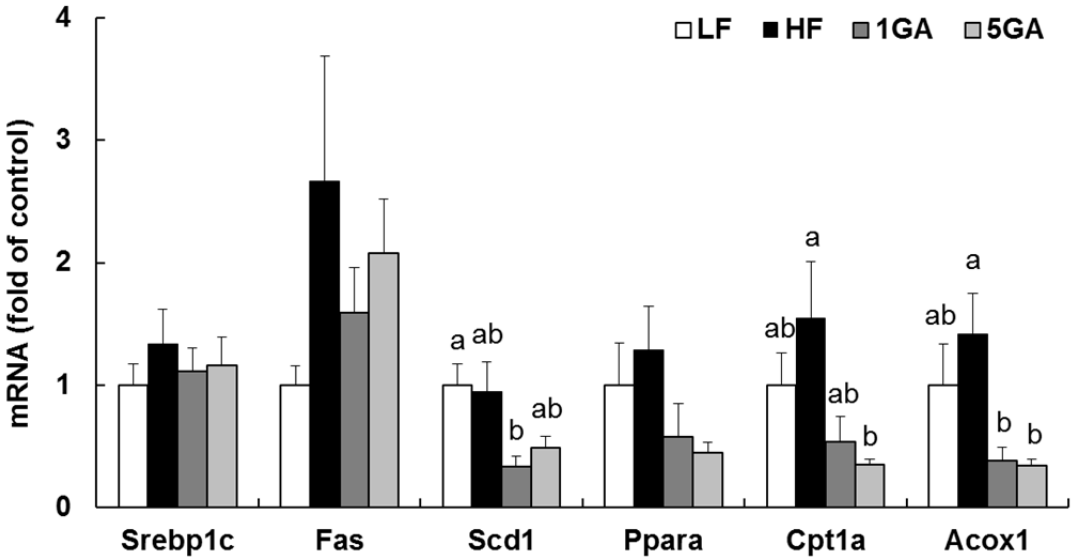

FIGURE 3-3 mRNA expression of the genes related to lipogenesis and fatty accid oxidation in the liver. Relative expression represented as fold of the LF group is shown. Values are

means ± SEMs, n = 6. Labeled means without a common letter are significantly different among groups at $P < 0.05$ as determined by Tukey's test. Abbreviations of each group are same as shown in **Fig. 3-1**.

Effects of dietary green alga on mRNA expression of genes related to lipid metabolism in adipose tissue

The effects of dietary green alga on the expression of adipogenic factors and lipid-regulating enzymes in WATs were investigated using real time RT-PCR method. In the mesenteric WAT, the mRNA levels of fatty acid synthesis-related genes, including *Srebp1c*, *Fas*, *Scd1* and glucose-6-phosphate dehydrogenase (*G6pd*) were measured. The mRNA expression of *Srebp1c*, *Fas*, *Scd1* and *G6pd* was significantly reduced in the 5GA group compared with the HF group (**Fig. 3-4A**). The 5% algal powder-supplemented diet significantly down-regulated the mRNA expression of peroxisome proliferator-activated receptor gamma (*Pparg*), which is a crucial transcription factor in adipogenesis, compared with the HF diet (**Fig. 3-4A**). Regarding the expression of fatty acid oxidation-related genes, the *Cpt1a* mRNA expression was not significantly different between the experimental groups, while the *Acox1* mRNA expression was significantly reduced in both algal powder supplemented-groups compared to the HF group. In contrast to the lipogenic genes analyzed, the mRNA expression of the energy expenditure-related gene PPAR gamma coactivator 1 alpha (*Pgc1a*) was significantly up-regulated in the 5GA group, while the mRNA expression of PPAR gamma coactivator 1 beta (*Pgc1b*) was not significantly different between HF group and the 5GA group.

In the perirenal WAT, the mRNA expression levels of lipogenic genes involving *Srebp1c*, *Fas*, *Scd1* and *G6pd* did not significantly differ between the GA and HF groups. Unlike in mesenteric WAT, in the perirenal WAT, *Pparg* expression was significantly enhanced in the 5GA group compared to the HF group (**Fig.3-4B**). In the perirenal WAT, *Cpt1a* expression

was significantly increased and *Acox1* expression tended to be higher ($P = 0.06$) in the 5GA group compared to the HF group; the expression of *Pgc1a* and *Pgc1b* was not significantly altered in 5GA group compared to the HF diet (**Fig. 3-4B**). In the epididymal WAT, the mRNA expression levels of above-mentioned genes evaluated in WATs were not significantly altered by algal powder supplementation compared to the HF diet (**Fig. 3-4C**). Moreover, the mRNA level of adiponectin (*Adipo*), the expression of which is decreased under conditions of obesity (92), was not significantly changed in all WATs in the GA group compared to the HF group. The mRNA expression of uncoupling protein 1 (*Ucp1*) in perirenal WAT was not changed between the GA groups and the HF group (Data not shown). The mRNA expression of *Ucp1* could not be detected in the mesenteric and epididymal WAT by real-time PCR.

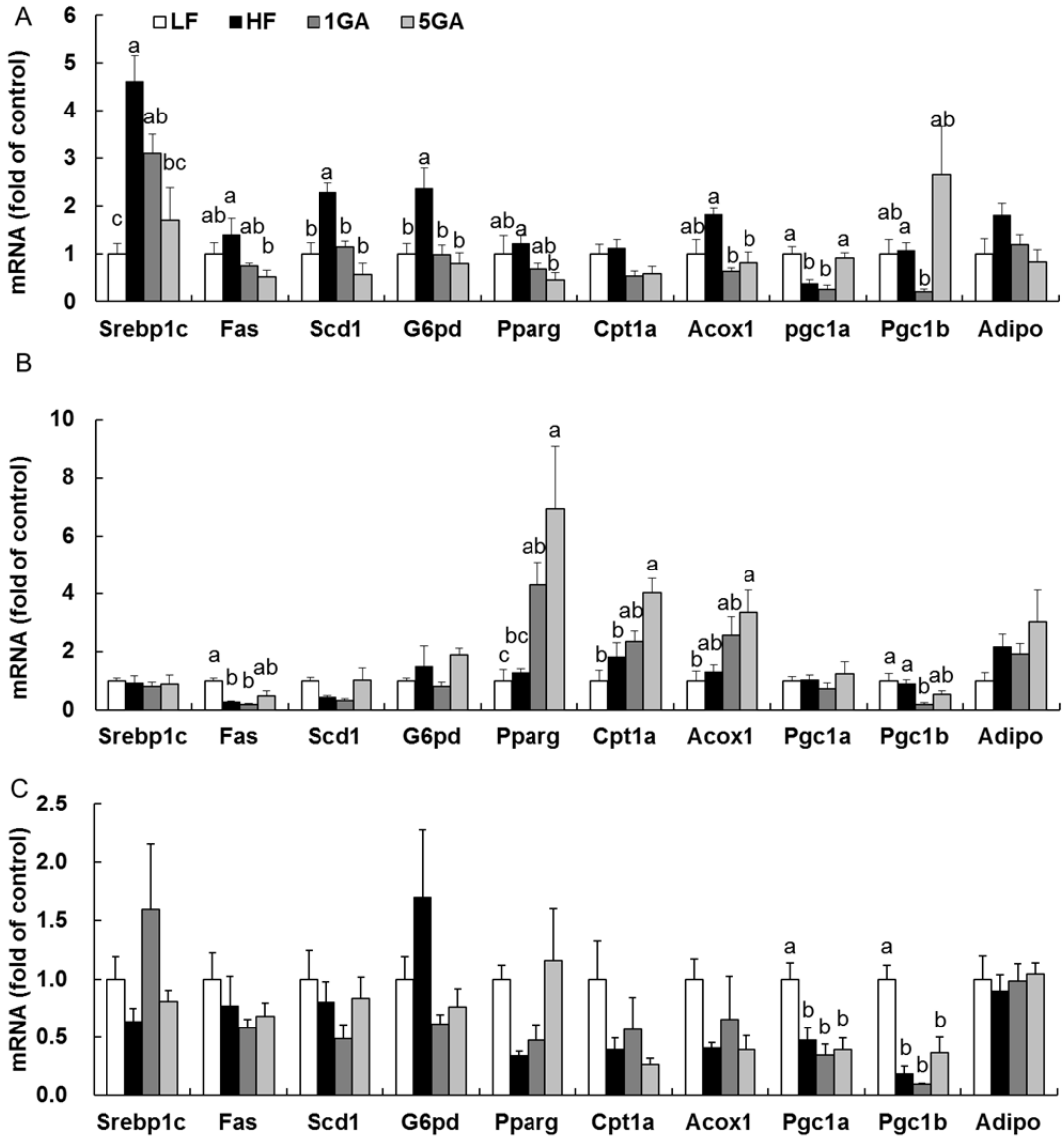

FIGURE 3-4 mRNA expression of lipid metabolic genes in the mesenteric WAT (A), perirenal WAT (B) and epididymal WAT (C). Relative expression represented as fold of the LF group is shown. Values are means ± SEMs, n = 6. Labeled means without a common letter are significantly different among groups at $P < 0.05$ as determined by Tukey's test. Abbreviations of each group are same as shown in **Fig. 3-1**.

Accumulation of siphonaxanthin in mesenteric WAT of mice fed green algal powder

The content of siphonaxanthin in *Codium cylindricum* used in this study was 230 μg/g, and neoxanthin, violaxanthin, lutein, siphonein and α-carotene were also detected (**Fig. 3-5B**). To evaluate the utilization efficiency of siphonaxanthin from dietary algal powder, the siphonaxanthin accumulation was investigated in adipose tissues and liver. Siphonaxanthin was found to accumulate in the mesenteric WAT following green algal powder supplementation (1.48 ± 0.20 and 5.57 ± 1.80 and ng/g tissues in 1GA and 5GA groups, respectively), although siphonaxanthin was not detected in the liver, perirenal WAT and epididymal WAT. Further, in order to understand the absorption efficiency of siphonaxanthin from dietary algal powder in mice, fecal excretion of siphonaxnathin were determined. The excretion of siphonaxanthin was calculated from the ratio of fecal siphonaxanthin content to siphonaxanthin intake for 24 h. The cumulative excretions of siphonaxanthin were 37.2 ± 1.3% and 57.6 ± 1.2% in 1GA and 5GA groups, respectively.

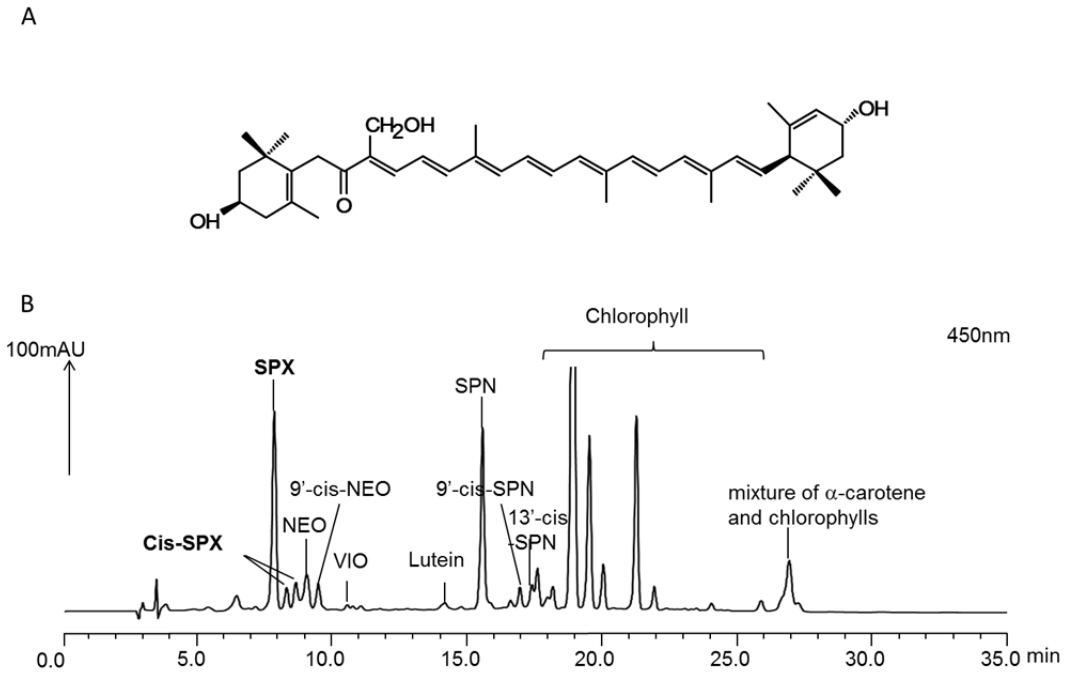

FIGURE 3-5 Chemical structure of siphonaxanthin (A), and HPLC chromatogram of extract of *Codium cylindricum* at 450 nm (B). NEO, neoxanthin; SPX, siphonaxanthin; SPN, siphonein; VIO, violaxanthin.

DISCUSSION

In this chapter, the effects of dietary-supplied green alga *Codium cylindricum* on the development of diet-induced obesity in C57BL/6J mice were evaluated. It was observed that dietary green alga significantly reduced high-fat diet-induced body weight gain and perirenal fat accumulation, and the dietary alga showed the tendency to reduce mesenteric and total WATs, and plasma cholesterol concentration. The present results show that dietary green alga also would be effective in improving diet-induced damage of liver, due to the restoration of both plasma AST and ALT to normal levels was observed.

The anti-obesity potential of edible algae has also been reported in several studies. For instance, Miyata *et al*. reported that dietary supplementation of tororokombu, an edible kelp product, inhibited fat absorption and lowered body weight and parauterine adipose tissue in obese mice induced by a high-fat diet for 63 d (90). It was reported that dietary supplementation of the brown alga *Sargassum polycystum* inhibited weight gain and ameliorated plasma lipids and glucose levels in rats fed a high-fat diet (91). The positive effect of these algae has been accounted for by the presence of a high amount of dietary fiber and anti-obesity active compounds, including carotenoids. However, the molecular mechanism underlying the inhibitory effect of these algae was uncertain.

The expression of adipogenic transcription factor (*Pparg*) and lipogenic transcription factor (*Srebp1c*), and their target genes (*Fas* and *Scd1*) were reported to be elevated in the adipose tissues of high-fat diet-induced mice, and several natural products possessing anti-obesity properties attenuates their expression (93-96). Likewise, dietary supplementation of the green alga also significantly reduced high-fat diet-induced the expression of lipogenic genes in the mesenteric WAT; however, the same effects were not observed in the perirenal and epididymal WATs. On the other hand, the enhancement of β-oxidation has been recognized as

one possible mechanism of prevention against obesity (18). *Cpt1a* and *Acox1* are rate-limiting enzymes which regulate fatty acid oxidation in the mitochondria (97, 98). High expression levels of *Cpt1a* and *Acox1* are consistent with increased triacylglycerol catabolism in liver and adipose tissue (99-101). In the study of this chapter, dietary green alga did not enhance the expression of β-oxidation genes in the mesenteric WAT, but instead prevented the increase of those by high-fat diet. While in the perirenal WAT, the 5% algal powder-supplemented diet significantly increased expression levels of *Cpt1a* and *Acox1*. *Pparg* is known as a most important pleiotropic transcription factors in the adipocyte differentiation, and its up-regulation is considered beneficial for the normalization of the functionality of endocrine adipose tissues to produce adipokins including adiponectin (102). In this study, the 5% algal powder-supplemented diet significantly increased the expression of *Pparg* in the perirenal WAT, while significantly decreased the expression of *Pparg* in the mesenteric WAT. The non-uniform effects of dietary green alga on synthetic and oxidative pathways of lipid among WATs might be due to the different anti-obesity mechanisms.

In this chapter, the aim is also to evaluate whether the bioactive carotenoid, siphonaxanthin, contributes to the prevention of obesity in mice orally supplemented with powdered green alga. In the chapter 1, it was found that the weight of visceral fat, especially the mesenteric WAT, was significantly reduced after oral administration with 1.3 mg siphonaxanthin for 6 weeks in diabetic KK-Ay mice (103). In order to understand the contribution of siphonaxanthin to the anti-obesity effect, the accumulation of siphonaxanthin in WATs of mice following supplementation of the green algal powder was further determined. The accumulation of siphonaxanthin was confirmed in the mesenteric WAT only, but was not in perirenal and epididymal WATs. Correspondently, these findings indicated that the down-regulation of lipogenesis-related gene expression in mesenteric WAT by supplementation of the green algal powder would be mainly caused by preferential accumulation of

siphonaxanthin. In fact, it was shown that siphonaxanthin administration to KK-Ay mice prevented the adiposity in the mesenteric WAT via the down-regulation of lipogenesis in chapter 1(103). The calculated average of dairy intake of siphonaxanthin in the experiment in this chapter (31.1 μg/day/mouse in 5GA group) is extremely lower compared to the dosage of the study of chapter 1 using sihonaxanthin concentrate (1.3 mg/day/mouse). In the present result, therefore, the weight of mesenteric WAT just tended to be lowered though lipogenic genes were down-regulated. In addition, absorption of siphonaxanthin from dietary alga was not efficient, because the excretion of siphonaxanthin for 24 h was more than approximately 40%. It was speculated that dietary fiber highly contained in the alga (70.7% in dried powder) could decrease the absorption of the carotenoid (71, 104). Thus, enhancement procedures for the bioavailability of siphonaxanthin might be more effective for exerting its potential.

It is generally known that marine algae contain many kinds of dietary fiber, the levels of which are more higher compared to terrestrial foodstuffs (105, 106). The main components of these dietary fibers are alginates, carrageenans, agar and so on, depending on the type of algae (105). Epidemiologic evidence suggests that dietary fiber intake aids in weight management via many mechanisms, including promoting satiety, decreasing absorption of fat, and altering secretion of gut hormones (107, 108). Some fibers found in algae have been reported to be associated with weight loss. For instance, sodium alginate from brown algae as a weight-loss supplement is widely considered worldwide (109, 110); fucoidan extracted from brown algae have been shown to have inhibitory effects on adipocyte differentiation (111, 112); and porphyran from the red alga have been shown to improve glucose metabolism and up-regulated plasma adiponectin concentration (113). Whereas, there has been no information about the potential anti-obesity effect of green algal polysaccharides. It was determined that the green alga *Codium cylindricum*, which was used in this chapter, contained 70.7% dietary fiber as dried powder (**Table 3-2**). The effect of dietary green alga on body weight loss might

partly be caused by the presence of high amount of soluble fiber, which helps to slow down digestion and fat absorption, in the alga. Dietary fiber has been reported to promote satiation by delaying gastric emptying and absorption of nutrients into the small intestine, and thus decrease food intake (108) However, algal powder supplementation did not affect food intake compared with the control HF diet group. Instead, the enhancement of feces weight, and fecal TG and NEFA concentration in the high dosage GA group was observed. The increase in fecal TG and TC, which means a decreased intestinal absorption of the lipids, can lead to the reduction of plasma and hepatic TG and TC concentration. Similarly, Miyata *et al.* reported that dietary brown algae, tororokombu, resulted in increased fecal TG and TC levels (90). The results may be explained by a presence of dietary fiber, which have been known as a good ingredient helping form large and soft stools, and slowing down the absorption of dietary fat (114, 115). The suppressive effect on the lipid absorption by dietary green alga might contribute to the weight loss of WATs, especially the perirenal WAT, in which the lipogenesis-related genes expression were not significantly altered.

In conclusion, the findings of this chapter indicated that supplementation with siphonaxanthin-rich green algae exerted anti-obesity effect. The dietary green alga reduced the WAT weight and ameliorated plasma and hepatic lipid profiles via the regulation of lipid metabolism in the adipose tissue and the inhibition of lipid absorption. These results revealed siphonaxanthin-rich green alga might be used as effective foodstuff to help prevent and control obesity.

SUMMARY AND CONCLUSION

In this study, siphonaxanthin isolated from green alga, *Codium cylindricum*, showed a potently inhibitory effect on the differentiation of 3T3-L1 preadipocytes. The inhibitory effect of siphonaxanthin on lipogenesis *in vivo* was investigated in diabetic KK-Ay mice. The possible molecular mechanisms underlying the anti-obesity effects of siphonaxanthin were elucidated. , In addition, the metabolism and tissues distribution of dietary siphonaxanthin were also examined, and siphonaxanthin and its metabolites were found largely accumulated in the mesenteric adipose tissue. Furthermore the possible role of siphonaxanthin in the anti-obesity effect of green algae was evaluated.

In chapter 1, compared to the other carotenoids evaluated, siphonaxanthin potently suppressed the differentiation of 3T3-L1 cells in a dose-dependent manner at non-cytotoxic concentrations. It was found that siphonaxanthin significantly lowered the expression of key adipogenesis genes, including *Cebpa*, *Pparg*, *Fabp4* and *Scd1*, almost to the levels observed in undifferentiated cells via inhibition of insulin-stimulated serine phosphorylation of Akt during adipogenesis. Moreover, oral administration of siphonaxanthin to KK-Ay mice significantly reduced the total weight of WAT, especially the mesenteric WAT.As the results of analysis of gene expression, it was indicated that dietary siphonaxanthin reduced lipogenesis and enhanced fatty acid oxidation in adipose tissue. In addition, siphonaxanthin was selectively accumulated in WATs, especially mesenteric WAT, and the accumulation in mesenteric WAT was approximately 2- and 3-fold of that in the epididymal and perirenal WAT, respectively.

In chapter 2, the absorption and biotransformation of siphonaxanthin were evaluated using intestinal Caco-2 cells. Furthermore, the tissue distribution and metabolic transformation of siphonaxanthin were evaluated in the ICR mice. The keto-carotenoids 3-oxo-siphonaxanthin,

3’-oxo-siphonaxanthin, and 3,3’-dioxo-siphonaxanthin were putatively identified as major metabolites in ICR mice after dietary administration of siphonaxanthin. The possible metabolic pathway for siphonaxanthin *in vivo* was as follows: siphonaxanthin to 3,3’-dioxo-siphonaxanthin (19-Hydroxy-7,8-dihydro-ε,ε-caroten-3,8,3’-trione) via 3-oxo-siphonaxanthin (19,3’-Dihydroxy-7,8-dihydro-β,ε-caroten-3,8-dione) or 3’-oxo-siphonaxanthin (3,19-Dihydroxy-7,8-dihydro-β,ε-caroten-8,3’-dione). Furthermore, it was found that siphonaxanthin and its metabolites exhibit a non-uniform accumulation and distribution pattern in tissues, and siphonaxanthin selectively accumulated in WAT, especially mesenteric WAT.

In chapter 3, the effect of siphonaxanthin-rich green alga *Codium cylindricum* on the development of high-fat diet-induced obesity in C57BL/6J mice was assessed. The mice were randomized to receive low-fat diet (LF; 7% fat, w/w), high-fat diet (HF; 35% fat, w/w), and high-fat diet supplemented with 1% and 5% green alga powder (1GA and 5GA) for 78 days. The results showed that the weights of body and perirenal WAT in 5GA group were significantly lower than that in the HF group. The mesenteric and total WAT, as well as plasma and hepatic cholesterol concentrations tended to be lower in both 1GA and 5GA group compared to the HF group. Furthermore, in the mesenteric WAT expression of lipogenesis-related genes, *Srebp1c*, *Fas*, *Scd1*, *G6pd* and *Pparg*, were significantly reduced in the 5GA group compared to the HF diet. Siphonaxanthin accumulated in the mesenteric WAT, which indicates that siphonaxanthin may be an important contributor to the down-regulation of lipogenesis in the mesenteric WAT. However, when alga powder containing siphoanxanthin was ingested, due to the poor abosorbtion of siphonaxanathin and its little accumulation in mesenteric WAT, the weight of mesenteric WAT was not significantly decreased. Furthermore, the enhancement of feces weight and fecal lipid concentration by algal powder

supplementation, which could result in the reduction in WATs weight, was attributed to the presence of dietary fiber in the green algae. In future, algal lipid extract, instead of algal powder, or the other processing methods may be more efficient for enhancement of siphonaxanthin absorption and exertion of anti-obesity activity of siphoanxanthin *in vivo*.

In conclusion, the present findings displayed a novel finding that siphonaxanthin and siphonaxanthin-rich green alga may be beneficial for the prevention of obesity and regulation of lipid metabolism. The possible molecular and metabolic mechanisms underlying its anti-obesity effects were elucidated. Although further efforts are needed to estimate its safety and effect in human, I believe that the study would provide a significant opportunity to develop and utilize the special carotenoid from green algae for nutraceutical or medicinal use.

ACKNOWLEDGEMENTS

I would like to give sincere thanks to a number of people who provided invaluable helps and encouragements through the road for the acquisition of the doctorate.

First and foremost, I would like to express my deepest appreciation and thanks to my supervisor Professor Dr. TATSUYA SUGAWARA, who have been a tremendous mentor for me. I appreciate all his contributions of time, ideas, and funding to make my Ph.D experience productive and stimulating. His invaluable suggestions, constructive criticisms, peerless guidance and kind encouragement, allow me to carry out the Ph.D research work successfully and grow as a research scientist.

I would also like to express my deepest gratitude to another supervisor of mine, Dr. TAKASHI HIRATA. He gave me opportunity to enter into the Kyoto University and start study for Ph.D. I would like to appreciate his warm-hearted encouragement, unselfish help, immense guidance and care, and spiritual motivation that help me to improve myself and overcome difficulties in my Ph.D research work. His advice on both research as well as on my career have been priceless and far-reaching to me.

I owe to my deepest appreciation to Dr. Yudong Cheng, professor of Shanghai Ocean University, China. He suggested the direction of my life by his professional experiences when I am a master student in China and supported me to apply for the Ph.D course in Kyoto University. I would like to thank for his continuous encouragement and care, even during my period of Japan.

I wish to thank all of the former and present members, especially assistant professor, Dr. YUKI MANABE, in the laboratory of Marine Bioproducts Technology, for their friendly

warm-hearted support during my stay in Japan and for their technical support and practical discussions and suggestion.

The financial support from the China scholarship council has been gratefully acknowledged. This support enabled me to concentrate my attention on the research and study.

Last but not least, a special thanks to my family. Words cannot express how grateful I am to my mother, father and husband for all of the sacrifices, care and love that they have made on my behalf. I would also like to thank all of my friends who supported and incented me to strive towards my goal in many ways. Due to their warm support, the research for doctor would be completed successfully.

REFERENCES

1. Das B, Srinivas KVNS. Bioactive Compounds from Red Algae of Marine Source. *Traditional Medicine* 1993: 349-51.

2. Mabeau S, Fleurence J. Seaweed in Food-Products - Biochemical and Nutritional Aspects. *Trends in Food Science & Technology* 1993; 4: 103-7.

3. Samarakoon K, Jeon YJ. Bio-functionalities of proteins derived from marine algae - A review. *Food Research International* 2012; 48: 948-60.

4. Holdt SL, Kraan S. Bioactive compounds in seaweed: functional food applications and legislation. *Journal of Applied Phycology* 2011; 23: 543-97.

5. Pangestuti R, Kim SK. Biological activities and health benefit effects of natural pigments derived from marine algae. *J Funct Foods* 2011; 3: 255-66.

6. Takaichi S. Carotenoids in algae: distributions, biosyntheses and functions. *Mar Drugs* 2011; 9: 1101-18.

7. Ikeuchi M, Koyama T, Takahashi J, Yazawa K. Effects of astaxanthin in obese mice fed a high-fat diet. *Biosci Biotechnol Biochem* 2007; 71: 893-9.

8. Bhuvaneswari S, Arunkumar E, Viswanathan P, Anuradha CV. Astaxanthin restricts weight gain, promotes insulin sensitivity and curtails fatty liver disease in mice fed a obesity-promoting diet. *Process Biochemistry* 2010; 45: 1406-14.

9. Woo MN, Jeon SM, Kim HJ, Lee MK, Shin SK, Shin YC, Park YB, Choi MS. Fucoxanthin supplementation improves plasma and hepatic lipid metabolism and blood glucose concentration in high-fat fed C57BL/6N mice. *Chem Biol Interact*

2010; 186: 316-22.

10. Ha AW, Kim WK. The effect of fucoxanthin rich power on the lipid metabolism in rats with a high fat diet. *Nutr Res Pract* 2013; 7: 287-93.

11. Maeda H, Hosokawa M, Sashima T, Murakami-Funayama K, Miyashita K. Anti-obesity and anti-diabetic effects of fucoxanthin on diet-induced obesity conditions in a murine model. *Mol Med Report* 2009; 2: 897-902.

12. Abidov M, Ramazanov Z, Seifulla R, Grachev S. The effects of Xanthigen (TM) in the weight management of obese premenopausal women with non-alcoholic fatty liver disease and normal liver fat. *Diabetes Obesity & Metabolism* 2010; 12: 72-81.

13. Ganesan P, Matsubara K, Ohkubo T, Tanaka Y, Noda K, Sugawara T, Hirata T. Anti-angiogenic effect of siphonaxanthin from green alga, Codium fragile. *Phytomedicine* 2010; 17: 1140-4.

14. Ganesan P, Matsubara K, Sugawara T, Hirata T. Marine algal carotenoids inhibit angiogenesis by down-regulating FGF-2-mediated intracellular signals in vascular endothelial cells. *Mol Cell Biochem* 2013; 380: 1-9.

15. Ganesan P, Noda K, Manabe Y, Ohkubo T, Tanaka Y, Maoka T, Sugawara T, Hirata T. Siphonaxanthin, a marine carotenoid from green algae, effectively induces apoptosis in human leukemia (HL-60) cells. *Biochim Biophys Acta* 2011; 1810: 497-503.

16. Browning JD, Horton JD. Molecular mediators of hepatic steatosis and liver injury. *J Clin Invest* 2004; 114: 147-52.

17. Despres JP. Health consequences of visceral obesity. *Ann Med* 2001; 33: 534-41.

18. Yun JW. Possible anti-obesity therapeutics from nature - A review. *Phytochemistry* 2010; 71: 1625-41.

19. Maeda H, Hosokawa M, Sashima T, Murakami-Funayama K, Miyashita K. Anti-obesity and anti-diabetic effects of fucoxanthin on diet-induced obesity conditions in a murine model. *Mol Med Rep* 2009; 2: 897-902.

20. Johnson EJ. The role of carotenoids in human health. *Nutr Clin Care* 2002; 5: 56-65.

21. Abidov M, Ramazanov Z, Seifulla R, Grachev S. The effects of Xanthigen in the weight management of obese premenopausal women with non-alcoholic fatty liver disease and normal liver fat. *Diabetes Obes Metab* 2010; 12: 72-81.

22. Asai A, Sugawara T, Ono H, Nagao A. Biotransformation of fucoxanthinol into amarouciaxanthin A in mice and HepG2 cells: Formation and cytotoxicity of fucoxanthin metabolites. *Drug Metabolism and Disposition* 2004; 32: 205-11.

23. Yim MJ, Hosokawa M, Mizushina Y, Yoshida H, Saito Y, Miyashita K. Suppressive effects of Amarouciaxanthin A on 3T3-L1 adipocyte differentiation through down-regulation of PPARgamma and C/EBPalpha mRNA expression. *J Agric Food Chem* 2011; 59: 1646-52.

24. Maeda H, Hosokawa M, Sashima T, Takahashi N, Kawada T, Miyashita K. Fucoxanthin and its metabolite, fucoxanthinol, suppress adipocyte differentiation in 3T3-L1 cells. *Int J Mol Med* 2006; 18: 147-52.

25. Bjorndal B, Burri L, Staalesen V, Skorve J, Berge RK. Different adipose depots: their role in the development of metabolic syndrome and mitochondrial response to hypolipidemic agents. *J Obes* 2011; 2011: 490650.

26. Hill JO, Peters JC. Environmental contributions to the obesity epidemic. *Science* 1998; 280: 1371-4.

27. Bray GA. Obesity: the disease. *J Med Chem* 2006; 49: 4001-7.

28. Bluher M. Adipose tissue dysfunction contributes to obesity related metabolic diseases. *Best Pract Res Clin Endocrinol Metab* 2013; 27: 163-77.

29. Gregoire FM, Smas CM, Sul HS. Understanding adipocyte differentiation. *Physiol Rev* 1998; 78: 783-809.

30. Ali AT, Hochfeld WE, Myburgh R, Pepper MS. Adipocyte and adipogenesis. *Eur J Cell Biol* 2013; 92: 229-36.

31. Lefterova MI, Lazar MA. New developments in adipogenesis. *Trends Endocrinol Metab* 2009; 20: 107-14.

32. Farmer SR. Transcriptional control of adipocyte formation. *Cell Metab* 2006; 4: 263-73.

33. Rosen ED, MacDougald OA. Adipocyte differentiation from the inside out. *Nat Rev Mol Cell Biol* 2006; 7: 885-96.

34. Gregoire FM. Adipocyte differentiation: from fibroblast to endocrine cell. *Exp Biol Med (Maywood)* 2001; 226: 997-1002.

35. Michaud EJ, Bultman SJ, Klebig ML, van Vugt MJ, Stubbs LJ, Russell LB, Woychik RP. A molecular model for the genetic and phenotypic characteristics of the mouse lethal yellow (Ay) mutation. *Proc Natl Acad Sci U S A* 1994; 91: 2562-6.

36. Iwatsuka H, Shino A, Suzuoki Z. General survey of diabetic features of yellow KK mice. *Endocrinol Jpn* 1970; 17: 23-35.

37. Herberg L, Coleman DL. Laboratory animals exhibiting obesity and diabetes syndromes. *Metabolism* 1977; 26: 59-99.

38. Maeda H, Hosokawa M, Sashima T, Funayama K, Miyashita K. Fucoxanthin from edible seaweed, Undaria pinnatifida, shows antiobesity effect through UCP1 expression in white adipose tissues. *Biochem Biophys Res Commun* 2005; 332: 392-7.

39. Beppu F, Hosokawa M, Niwano Y, Miyashita K. Effects of dietary fucoxanthin on cholesterol metabolism in diabetic/obese KK-A(y) mice. *Lipids Health Dis* 2012; 11.

40. Jeon SM, Kim HJ, Woo MN, Lee MK, Shin YC, Park YB, Choi MS. Fucoxanthin-rich seaweed extract suppresses body weight gain and improves lipid metabolism in high-fat-fed C57BL/6J mice. *Biotechnol J* 2010; 5: 961-9.

41. Woo MN, Jeon SM, Shin YC, Lee MK, Kang MA, Choi MS. Anti-obese property of fucoxanthin is partly mediated by altering lipid-regulating enzymes and uncoupling proteins of visceral adipose tissue in mice. *Mol Nutr Food Res* 2009; 53: 1603-11.

42. Walton TJ, Britton G, Goodwin TW. The structure of siphonaxanthin. *Phytochemistry* 1973; 9: 2545-52.

43. Sugawara T, Ganesan P, Li Z, Manabe Y, Hirata T. Siphonaxanthin, a green algal carotenoid, as a novel functional compound. *Mar Drugs* 2014; 12: 3660-8.

44. Manabe Y, Hirata T, Sugawara T. Suppressive Effects of Carotenoids on the Antigen-induced Degranulation in RBL-2H3 Rat Basophilic Leukemia Cells. *J Oleo Sci* 2014;

63: 291-4.

45. Reeves PG, Nielsen FH, Fahey GC, Jr. AIN-93 purified diets for laboratory rodents: final report of the American Institute of Nutrition ad hoc writing committee on the reformulation of the AIN-76A rodent diet. *J Nutr* 1993; 123: 1939-51.

46. Shan T, Liu W, Kuang S. Fatty acid binding protein 4 expression marks a population of adipocyte progenitors in white and brown adipose tissues. *FASEB J* 2013; 27: 277-87.

47. Ntambi JM, Buhrow SA, Kaestner KH, Christy RJ, Sibley E, Kelly TJ, Jr., Lane MD. Differentiation-induced gene expression in 3T3-L1 preadipocytes. Characterization of a differentially expressed gene encoding stearoyl-CoA desaturase. *J Biol Chem* 1988; 263: 17291-300.

48. Garofalo RS, Orena SJ, Rafidi K, Torchia AJ, Stock JL, Hildebrandt AL, Coskran T, Black SC, Brees DJ, Wicks JR, et al. Severe diabetes, age-dependent loss of adipose tissue, and mild growth deficiency in mice lacking Akt2/PKB beta. *J Clin Invest* 2003; 112: 197-208.

49. Xu J, Liao K. Protein kinase B/AKT 1 plays a pivotal role in insulin-like growth factor-1 receptor signaling induced 3T3-L1 adipocyte differentiation. *J Biol Chem* 2004; 279: 35914-22.

50. Kohn AD, Summers SA, Birnbaum MJ, Roth RA. Expression of a constitutively active Akt Ser/Thr kinase in 3T3-L1 adipocytes stimulates glucose uptake and glucose transporter 4 translocation. *J Biol Chem* 1996; 271: 31372-8.

51. Hamm JK, Park BH, Farmer SR. A role for C/EBPbeta in regulating peroxisome

proliferator-activated receptor gamma activity during adipogenesis in 3T3-L1 preadipocytes. *J Biol Chem* 2001; 276: 18464-71.

52. Tang QQ, Gronborg M, Huang H, Kim JW, Otto TC, Pandey A, Lane MD. Sequential phosphorylation of CCAAT enhancer-binding protein beta by MAPK and glycogen synthase kinase 3beta is required for adipogenesis. *Proc Natl Acad Sci U S A* 2005; 102: 9766-71.

53. Tang QQ, Otto TC, Lane MD. CCAAT/enhancer-binding protein beta is required for mitotic clonal expansion during adipogenesis. *Proc Natl Acad Sci U S A* 2003; 100: 850-5.

54. Shirakura Y, Takayanagi K, Mukai K, Tanabe H, Inoue M. beta-cryptoxanthin suppresses the adipogenesis of 3T3-L1 cells via RAR activation. *J Nutr Sci Vitaminol (Tokyo)* 2011; 57: 426-31.

55. Kim CY, Le TT, Chen C, Cheng JX, Kim KH. Curcumin inhibits adipocyte differentiation through modulation of mitotic clonal expansion. *J Nutr Biochem* 2011; 22: 910-20.

56. Okada T, Nakai M, Maeda H, Hosokawa M, Sashima T, Miyashita K. Suppressive effect of neoxanthin on the differentiation of 3T3-L1 adipose cells. *J Oleo Sci* 2008; 57: 345-51.

57. Harmon AW, Patel YM, Harp JB. Genistein inhibits CCAAT/enhancer-binding protein beta (C/EBPbeta) activity and 3T3-L1 adipogenesis by increasing C/EBP homologous protein expression. *Biochem J* 2002; 367: 203-8.

58. Lee J, Kim D, Choi J, Choi H, Ryu JH, Jeong J, Park EJ, Kim SH, Kim S.

Dehydrodiconiferyl alcohol isolated from Cucurbita moschata shows anti-adipogenic and anti-lipogenic effects in 3T3-L1 cells and primary mouse embryonic fibroblasts. *J Biol Chem* 2012; 287: 8839-51.

59. Maeda H, Hosokawa M, Sashima T, Miyashita K. Dietary combination of fucoxanthin and fish oil attenuates the weight gain of white adipose tissue and decreases blood glucose in obese/diabetic KK-Ay mice. *J Agric Food Chem* 2007; 55: 7701-6.

60. Strable MS, Ntambi JM. Genetic control of de novo lipogenesis: role in diet-induced obesity. *Crit Rev Biochem Mol Biol* 2010; 45: 199-214.

61. Enguix N, Pardo R, Gonzalez A, Lopez VM, Simo R, Kralli A, Villena JA. Mice lacking PGC-1beta in adipose tissues reveal a dissociation between mitochondrial dysfunction and insulin resistance. *Mol Metab* 2013; 2: 215-26.

62. Semple RK, Crowley VC, Sewter CP, Laudes M, Christodoulides C, Considine RV, Vidal-Puig A, O'Rahilly S. Expression of the thermogenic nuclear hormone receptor coactivator PGC-1 alpha is reduced in the adipose tissue of morbidly obese subjects. *Int J Obes* 2004; 28: 176-9.

63. Boss O, Samec S, Desplanches D, Mayet MH, Seydoux J, Muzzin P, Giacobino JP. Effect of endurance training on mRNA expression of uncoupling proteins 1, 2, and 3 in the rat. *FASEB J* 1998; 12: 335-9.

64. Clapham JC, Arch JRS, Chapman H, Haynes A, Lister C, Moore GBT, Piercy V, Carter SA, Lehner I, Smith SA, et al. Mice overexpressing human uncoupling protein-3 in skeletal muscle are hyperphagic and lean. *Nature* 2000; 406: 415-8.

65. Nakano R, Kurosaki E, Yoshida S, Yokono M, Shimaya A, Maruyama T, Shibasaki M.

Antagonism of peroxisome proliferator-activated receptor gamma prevents high-fat diet-induced obesity in vivo. *Biochem Pharmacol* 2006; 72: 42-52.

66. Foote CS, Chang YC, Denny RW. Chemistry of singlet oxygen. XI. Cis-trans isomerization of carotenoids by singlet oxygen and a probable quenching mechanism. *J Am Chem Soc* 1970; 92: 5218-9.

67. Martin HD, Ruck C, Schmidt M, Sell S, Beutner S, Mayer B, Walsh R. Chemistry of carotenoid oxidation and free radical reactions. *Pure Appl Chem* 1999; 71: 2253-62.

68. Fiedor J, Burda K. Potential Role of Carotenoids as Antioxidants in Human Health and Disease. *Nutrients* 2014; 6: 466-88.

69. Riccioni G. Marine carotenoids and oxidative stress. *Mar Drugs* 2012; 10: 116-8.

70. Thomson CA, Stendell-Hollis NR, Rock CL, Cussler EC, Flatt SW, Pierce JP. Plasma and dietary carotenoids are associated with reduced oxidative stress in women previously treated for breast cancer. *Cancer Epidemiol Biomarkers Prev* 2007; 16: 2008-15.

71. Hof KHV, West CE, Weststrate JA, Hautvast JGAJ. Dietary factors that affect the bioavailability of carotenoids. *J Nutr* 2000; 130: 503-6.

72. Yonekura L, Nagao A. Intestinal absorption of dietary carotenoids. *Mol Nutr Food Res* 2007; 51: 107-15.

73. Furr HC, Clark RM. Intestinal absorption and tissue distribution of carotenoids. *Journal of Nutritional Biochemistry* 1997; 8: 364-77.

74. Parker RS. Carotenoids in human blood and tissues. *J Nutr* 1989; 119: 101-4.

75. Borchardt RT. Hidalgo, I. J., Raub, T. J., and Borchardt, R. T.: Characterization of the Human Colon Carcinoma Cell Line (Caco-2) as a Model System for Intestinal Epithelial Permeability, Gastroenterology, 96, 736-749, 1989-The Backstory. *Aaps Journal* 2011; 13: 323-7.

76. Hidalgo IJ, Raub TJ, Borchardt RT. Characterization of the Human-Colon Carcinoma Cell-Line (Caco-2) as a Model System for Intestinal Epithelial Permeability. *Gastroenterology* 1989; 96: 736-49.

77. Pinto M, Robineleon S, Appay MD, Kedinger M, Triadou N, Dussaulx E, Lacroix B, Simonassmann P, Haffen K, Fogh J, et al. Enterocyte-Like Differentiation and Polarization of the Human-Colon Carcinoma Cell-Line Caco-2 in Culture. *Biology of the Cell* 1983; 47: 323-30.

78. Biganzoli E, Cavenaghi LA, Rossi R, Brunati MC, Nolli ML. Use of a Caco-2 cell culture model for the characterization of intestinal absorption of antibiotics. *Farmaco* 1999; 54: 594-9.

79. Sugawara T, Kushiro M, Zhang H, Nara E, Ono H, Nagao A. Lysophosphatidylcholine enhances carotenoid uptake from mixed micelles by Caco-2 human intestinal cells. *J Nutr* 2001; 131: 2921-7.

80. Yonekura L, Kobayashi M, Terasaki M, Nagao A. Keto-Carotenoids Are the Major Metabolites of Dietary Lutein and Fucoxanthin in Mouse Tissues. *J Nutr* 2010; 140: 1824-31.

81. Etoh H, Utsunomiya Y, Komori A, Murakami Y, Oshima S, Inakuma T. Carotenoids in human blood plasma after ingesting paprika juice. *Bioscience Biotechnology and*

Biochemistry 2000; 64: 1096-8.

82. Zeng S, Furr HC, Olson JA. Human metabolism of carotenoid analogs and apocarotenoids. *Methods Enzymol* 1993; 214: 137-47.

83. Sugawara T, Yamashita K, Asai A, Nagao A, Shiraishi T, Imai I, Hirata T. Esterification of xanthophylls by human intestinal Caco-2 cells. *Arch Biochem Biophys* 2009; 483: 205-12.

84. Khachik F, de Moura FF, Chew EY, Douglass LW, Ferris FL, 3rd, Kim J, Thompson DJ. The effect of lutein and zeaxanthin supplementation on metabolites of these carotenoids in the serum of persons aged 60 or older. *Invest Ophthalmol Vis Sci* 2006; 47: 5234-42.

85. Khachik F. Distribution and metabolism of dietary carotenoids in humans as a criterion for development of nutritional supplements. *Pure Appl Chem* 2006; 78: 1551-7.

86. Nagao A. Bioavailability of Dietary Carotenoids: Intestinal Absorption and Metabolism. *Jarq-Japan Agricultural Research Quarterly* 2014; 48: 385-91.

87. Hashimoto T, Ozaki Y, Taminato M, Das SK, Mizuno M, Yoshimura K, Maoka T, Kanazawa K. The distribution and accumulation of fucoxanthin and its metabolites after oral administration in mice. *Br J Nutr* 2009; 102: 242-8.

88. Murakami A, Takahashi D, Kinoshita T, Koshimizu K, Kim HW, Yoshihiro A, Nakamura Y, Jiwajinda S, Terao J, Ohigashi H. Zerumbone, a Southeast Asian ginger sesquiterpene, markedly suppresses free radical generation, proinflammatory protein production, and cancer cell proliferation accompanied by apoptosis: the alpha,beta-

unsaturated carbonyl group is a prerequisite. *Carcinogenesis* 2002; 23: 795-802.

89. Ha AW, Kim WK. The effect of fucoxanthin rich power on the lipid metabolism in rats with a high fat diet. *Nutrition Research and Practice* 2013; 7: 287-93.

90. Miyata M, Koyama T, Kamitani T, Toda T, Yazawa K. Anti-Obesity Effect on Rodents of the Traditional Japanese Food, Tororokombu, Shaved Laminaria. *Bioscience Biotechnology and Biochemistry* 2009; 73: 2326-8.

91. Awang AN, Ng JL, Matanjun P, Sulaiman MR, Tan TS, Ooi YBH. Anti-obesity property of the brown seaweed, Sargassum polycystum using an in vivo animal model. *Journal of Applied Phycology* 2014; 26: 1043-8.

92. Barnea M, Shamay A, Stark AH, Madar Z. A high-fat diet has a tissue-specific effect on adiponectin. and related enzyme expression. *Obesity* 2006; 14: 2145-53.

93. Jung CH, Ahn J, Jeon TI, Kim TW, Ha TY. Syzygium aromaticum ethanol extract reduces high-fat diet-induced obesity in mice through downregulation of adipogenic and lipogenic gene expression. *Exp Ther Med* 2012; 4: 409-14.

94. Kim S, Jin Y, Choi Y, Park T. Resveratrol exerts anti-obesity effects via mechanisms involving down-regulation of adipogenic and inflammatory processes in mice. *Biochem Pharmacol* 2011; 81: 1343-51.

95. Choi HJ, Eo H, Park K, Jin M, Park EJ, Kim SH, Park JE, Kim S. A water-soluble extract from Cucurbita moschata shows anti-obesity effects by controlling lipid metabolism in a high fat diet-induced obesity mouse model. *Biochem Biophys Res Commun* 2007; 359: 419-25.

96. Lee H, Kang R, Yoon Y. SH21B, an anti-obesity herbal composition, inhibits fat accumulation in 3T3-L1 adipocytes and high fat diet-induced obese mice through the modulation of the adipogenesis pathway. *J Ethnopharmacol* 2010; 127: 709-17.

97. Lee K, Kerner J, Hoppel CL. Mitochondrial Carnitine Palmitoyltransferase 1a (CPT1a) Is Part of an Outer Membrane Fatty Acid Transfer Complex. *J Biol Chem* 2011; 286: 25655-62.

98. Vluggens A, Andreoletti P, Viswakarma N, Jia Y, Matsumoto K, Kulik W, Khan M, Huang J, Guo D, Yu S, et al. Reversal of mouse Acyl-CoA oxidase 1 (ACOX1) null phenotype by human ACOX1b isoform [corrected]. *Lab Invest* 2010; 90: 696-708.

99. Novak EM, Keller BO, Innis SM. Metabolic development in the liver and the implications of the n-3 fatty acid supply. *American Journal of Physiology-Gastrointestinal and Liver Physiology* 2012; 302: G250-G9.

100. Jeon SM, Kim HJ, Woo MN, Lee MK, Shin YC, Park YB, Choi MS. Fucoxanthin-rich seaweed extract suppresses body weight gain and improves lipid metabolism in high-fat-fed C57BL/6J mice. *Biotechnol J* 2010; 5: 961-9.

101. Seo KI, Lee J, Choi RY, Lee HI, Lee JH, Jeong YK, Kim MJ, Lee MK. Anti-obesity and anti-insulin resistance effects of tomato vinegar beverage in diet-induced obese mice. *Food & Function* 2014; 5: 1579-86.

102. Rizzo G, Disante M, Mencarelli A, Renga B, Gioiello A, Pellicciari R, Fiorucci S. The farnesoid X receptor promotes adipocyte differentiation and regulates adipose cell function in vivo. *Mol Pharmacol* 2006; 70: 1164-73.

103. Li ZS NK, Fujita E, Manabe Y, Hirata T, and Sugawara T. The Green Algal Carotenoid

Siphonaxanthin Inhibits Adipogenesis in 3T3-L1 Preadipocytes and the Accumulation of Lipids in White Adipose Tissue of KK-Ay Mice. *J Nutr* 2015.

104. Yonekura L, Nagao A. Intestinal absorption of dietary carotenoids. *Mol Nutr Food Res* 2007; 51: 107-15.

105. MacArtain P, Gill CIR, Brooks M, Campbell R, Rowland IR. Nutritional value of edible seaweeds. *Nutr Rev* 2007; 65: 535-43.

106. Gomez-Ordonez E, Jimenez-Escrig A, Ruperez P. Dietary fibre and physicochemical properties of several edible seaweeds from the northwestern Spanish coast. *Food Research International* 2010; 43: 2289-94.

107. Lairon D. Dietary fiber and control of body weight. *Nutrition Metabolism and Cardiovascular Diseases* 2007; 17: 1-5.

108. Slavin JL. Dietary fiber and body weight. *Nutrition* 2005; 21: 411-8.

109. Odunsi ST, Vazquez-Roque MI, Camilleri M, Papathanasopoulos A, Clark MM, Wodrich L, Lempke M, McKinzie S, Ryks M, Burton D, et al. Effect of Alginate on Satiation, Appetite, Gastric Function, and Selected Gut Satiety Hormones in Overweight and Obesity. *Obesity* 2010; 18: 1579-84.

110. Dettmar PW, Strugala V, Richardson JC. The key role alginates play in health. *Food Hydrocolloids* 2011; 25: 263-6.

111. Kim MJ, Chang UJ, Lee JS. Inhibitory Effects of Fucoidan in 3T3-L1 Adipocyte Differentiation. *Marine Biotechnology* 2009; 11: 557-62.

112. Kim KJ, Lee OW, Lee BY. Fucoidan, a sulfated polysaccharide, inhibits adipogenesis

through the mitogen-activated protein kinase pathway in 3T3-L1 preadipocytes. *Life Sci* 2010; 86: 791-7.

113. Kitano Y, Murazumi K, Duan JJ, Kurose K, Kobayashi S, Sugawara T, Hirata T. Effect of Dietary Porphyran from the Red Alga, Porphyra yezoensis, on Glucose Metabolism in Diabetic KK-Ay Mice. *J Nutr Sci Vitaminol (Tokyo)* 2012; 58: 14-9.

114. Du H, van der AD, Boshuizen HC, Forouhi NG, Wareham NJ, Halkjaer J, Tjonneland A, Overvad K, Jakobsen MU, Boeing H, et al. Dietary fiber and subsequent changes in body weight and waist circumference in European men and women. *Am J Clin Nutr* 2010; 91: 329-36.

115. Burkitt DP, Walker AR, Painter NS. Effect of dietary fibre on stools and the transit-times, and its role in the causation of disease. *Lancet* 1972; 2: 1408-12.